
Integrated approach for zonation of a mid-Cenomanian carbonate reservoir in a sequence stratigraphic framework

R. JODEYRI-AGAH¹ H. RAHIMPOUR-BONAB^{1*} V. TAVAKOLI¹ R. KADKHOAIE-ILKHCHI² M.-R. YOUSEFPOOR³

¹School of Geology, College of Science, University of Tehran

14176-14411, Tehran (Iran). Jodeyri-Agahi E-mail: jodeyri_rana@yahoo.com
Rahimpour-Bonab E-mail: rahimpor@ut.ac.ir Tavakoli E-mail: vtavakoli@ut.ac.ir

²Department of Earth Science, Faculty of Natural Science, University of Tabriz

29 Bahman Boulevard, No. 51666, Tabriz (Iran). E-mail: rahimkadkhodaee2005@yahoo.com

³Exploration projects management, Iranian Offshore Oil Company

Valiassar Street, Toraj Alley, No. 12, Tehran (Iran) E-mail: myousefpoor@iooc.co.ir

*Corresponding author

| A B S T R A C T |

The mid-Cenomanian Mishrif Formation (Fm.) is considered as one of the most important rudist-bearing reservoir horizons in the Sirri Oil Fields of the Persian Gulf. Due to the general heterogeneity of carbonate reservoirs, the use of an integrated approach is helpful for investigating porosity and permeability distribution along with recognizing controlling pore system factors in the reservoir. Thus, for the reservoir characterization of the Mishrif Fm., an integrated approach including facies analysis, diagenetic history and sequence stratigraphic analysis is considered. Detailed petrographic studies showed a total of eight microfacies and seven facies belts, related to inner ramp to the basin of a homoclinal carbonate ramp. Humid climatic condition and tectonic activity, associated with eustatic sea-level fluctuations during the mid-Cretaceous, led to meteoric diagenesis of the Mishrif carbonates during subaerial exposures (mid-Cenomanian and Cenomanian-Turonian disconformities). General diagenetic overprints and modifications include micritization, cementation, dissolution, compaction, dolomitization, pyritization and fracturing. Considering this reservoir in the sequence stratigraphic framework reveals that the reservoir zones development is basically related to the Cenomanian–Turonian sequence boundary, recognized in the three studied wells, and also to the mid-Cenomanian boundary, identified only in one well. In addition, pore system properties were inspected by differentiation of Hydraulic Flow Units (HFUs) within the reservoir. The identified flow units, based on their capability for fluid flow, can be classified into four main rock types with very high- (HFUD), high- (HFUC), medium- (HFUB) and low-quality (HFUA). Accordingly, this study shows that the main part of the Mishrif Reservoir is affected by diagenetic processes related to subaerial exposures, resulting in zones with higher storage capacity and fluid flow rates. So, the study of depositional and diagenetic characteristics of the Mishrif carbonates in the sequence stratigraphy framework is essential to unravel the reservoir heterogeneity, and to describe the reservoir zones and their distribution in the field and regional scale. In addition, observed changes in the thickness of hydrocarbon column are attributed to the different location of the studied wells on the anticline structures, which show a tilted oil-water contact with a slope to the North.

KEYWORDS

Reservoir characteristics. Flow units. Sequence stratigraphy. Mishrif Formation. Sirri Field. Reservoir zonation.

INTRODUCTION

Hydrocarbon accumulations of the Albian–Turonian carbonate sequences in the Arabian Plate have been mostly developed on epeiric carbonate platforms, located in the passive margins of the Neotethys Ocean. These sequences have been developed from Iraq in the North to Oman in the South, Arabia in the West and Iran in the East, as it covering an area more than 1000km-long from the South towards the North and North-West of the Arabian Plate (Van Buchem *et al.*, 1996; Droste and Van Steenwinkel, 2004). A significant portion of the petroleum reserves of this time interval in the Central-East and the Persian Gulf is hosted in carbonates. Generally, several factors including eustatic sea-level fluctuations and humid climate mainly controlled depositional facies changes and the subaerial exposures as well as the near-surface diagenetic events. These parameters ultimately constructed the overall anatomy and geometry of the carbonate reservoirs (Hollis, 2011).

In this carbonate sequence, deposited under warm humid climatic conditions, the effects of early diagenetic events are typically related to high-rate of meteoric waters circulation, shaping the ultimate reservoir characteristics (Petty, 2005; Ehrenberg *et al.*, 2007; Hollis, 2011). In this context, development of dissolution vugs and karstification resulted in the improved reservoir quality (Mazzullo and Chilingarian, 1992). Thus, presence of the subaerial exposures, associated with meteoric water circulations, control the pore system properties and its distribution within the reservoir (Harris *et al.*, 1984; Mazzullo and Chilingarian, 1992; Weidlich, 2010). On the other hand, the effect of burial dissolution on the development of vugs and enhancement of reservoir quality is not negligible (Harris *et al.*, 1984; Sun and Esteban, 1994; Ehrenberg *et al.*, 2007; Razin *et al.*, 2010; Weidlich, 2010). Therefore, determination of the paragenetic sequence provides some information on porosity and permeability development and the factors controlling the reservoir quality (Moore, 2001; Al-Habashi *et al.*, 2003; Rahimpour-Bonab, 2007; Ahr, 2008).

The middle Cenomanian Mishrif Formation (Fm.) hosted several important hydrocarbon reserves in the Persian Gulf, including Sirri Oil fields. The formation in the Sirri Oil fields consists of carbonate units deposited under the dominance of humid climatic condition of the middle Cretaceous. These carbonates underwent subaerial exposure and so are affected by significant meteoric diagenesis (Al-Kharsan, 1975; Alsharhan and Nairn, 1988; Alsharhan and Kendall, 1991; Alsharhan, 1995; Al-Mohammad, 2012, Assadi *et al.*, 2016). Thus, illustrating facies distribution and diagenetic events of this formation in the sequence stratigraphic framework could help us to

understand the reservoir zones distribution in these fields, and to recognize the main factors controlling reservoir properties of the Mishrif carbonates. Thus, main goals of this paper are summarized as follows:

i) Reconstructing a three-dimensional conceptual depositional model for the Mishrif Platform based on the distribution and frequency of the recognized sedimentary facies in the studied fields.

ii) Recognition of diagenetic processes and their effects on reservoir quality of the Mishrif, so depicting diagenetic events in a paragenetic sequence.

iii) Analyzing sequence stratigraphy of this unit on the transgressive-regressive sequence model (T–R sequence), Embry and Johansson, 1992.

iv) Determining Hydraulic Flow Units (HFUs) based on Flow Zone Indicator (FZI) method (Amaefule *et al.*, 1993) and depicting flow units distributions within the reservoir interval by considering the facies variations and main diagenetic overprints, portrayed in the general sequence stratigraphic framework.

v) Finally, using the water saturation parameters for thickness, estimation of hydrocarbon column and investigating its variation among the studied wells of the Sirri fields.

GEOLOGICAL SETTING AND STRATIGRAPHY

In the Persian Gulf, the association of porous and permeable reservoir units with the different prolific source rocks led to the formation of significant hydrocarbon reserves. In addition, numerous tectonic structures such as anticlines, salt domes and diapirs associated with effective cap rocks provided the suitable conditions for hydrocarbon entrapment (Ghazban and Motiei, 2010).

In a large-scale, the Cretaceous sequence is divided into two stratigraphy-structural mega-sequences (AP8 and AP9) (Sharland *et al.*, 2001). The total Albian to Turonian interval of the Arabian Plate is included in AP8 mega-sequence, which has been confined by maximum flooding surfaces (K140– K90) (Sharland *et al.*, 2001; Davies *et al.*, 2002) (Fig. 1, Electronic Appendix available at www.geologica-acta.com). Wasia Group includes the upper part of the mega-sequence AP8 (Ehrenberg *et al.*, 2008). The top of this mega-sequence is distinguished by the extensive mid-Turonian disconformity (the boundary between Wasia and Aruma groups). Near the margin of paleo-platform, the Albian to Cenomanian interval consists of shallow water carbonates deposited under low- to medium-energy

conditions and water depth of about 10m or less (Burchette and Britton, 1985; Jordan *et al.*, 1985; Burchette, 1993; Philip *et al.*, 1995; Van Buchem *et al.*, 1996, 2002).

During the Cretaceous, the interaction between eustasy (continuous global sea-level rising) and humid climate condition played an important role in the depositional-diagenetic history of the Arabian Platform (Blanc *et al.*, 2003; McQuarrie, 2004; Sherkati and Letouzey, 2004; Sepehr and Cosgrove, 2005; Sherkati *et al.*, 2005; Rahimpour-Bonab *et al.*, 2009; Hollis, 2011). The interplay of these factors during the Cenomanian to Turonian led to the occurrence of three disconformities of mid-Cenomanian, late-Cenomanian–Turonian and mid-Turonian (Blanc *et al.*, 2003; Verges *et al.*, 2009; Emami *et al.*, 2010; Aqrabi *et al.*, 2010; Sharp *et al.*, 2010; Razin *et al.*, 2010; Hollis, 2011). The mid-Cenomanian and mid-Turonian disconformities are present in the regional scale (Alsharhan and Nairn, 1986, 1988; Motiei, 1993; Aqrabi *et al.*, 1998, 2010).

The mid-Cretaceous sequences in the southern part of the Persian Gulf include the Wasia Group consisting the Nahr-Umr, Khatiyah and Mishrif formations from base to top of the sequence (Fig. 1). The Wasia Group has been deposited in periods of more than 20Ma, in a progradational system, beginning with deposition of a neritic layer (Ghazban and Motiei, 2010). Shales, siltstones and sandstones of this group overlay the lower Cretaceous Tamamas Group. This trend indicates an upwards change

from clastic to shallow carbonate shelf. In addition, deep-marine carbonates of the intra-shelf basin are involved in this group (Ghazban and Motiei, 2010).

The Cenomanian sequence of the Persian Gulf is composed of intra-basinal carbonates of the early Cenomanian Khatiya Fm. (the equivalent of Ahmadi Fm. in Zagros) which is followed by deposition of shallow-water carbonates of the Mishrif Fm. (the equivalent of the upper part of the Mishrif Fm. in Zagros). The mid-Cenomanian Mishrif Fm. consists of a progradational sedimentary sequence considered as an important oil-producing interval in the Persian Gulf. The shallow-water carbonates of this sequence in the southern Persian Gulf prograde, in some areas more than 75m, into the basin (Burchette, 1993). This carbonate formation involves both shallow-marine (with rudist skeletal grains and benthic foraminifera) and deeper-marine (with planktonic foraminifera) facies (Burchette, 1993). Development of high-quality reservoir zones within the formation is related to several factors including depositional facies (abundance of rudists) and the action of diagenesis (percolation of meteoric waters) under the effect of the mid-Cretaceous eustatic sea-level fluctuations associated with the dominance of tropical climate (Mehrabi and Rahimpour-Bonab, 2014; Mehrabi *et al.*, 2015). These resulted in the development of dissolution vugs and karstification during periods of subaerial exposures. The Mishrif Fm. is considered as one of the most important rudist-bearing reservoir horizons in the Sirri oil fields of Iran and Fateh Oil Field in the United Arab Emirates (Ghazban and Motiei, 2010).

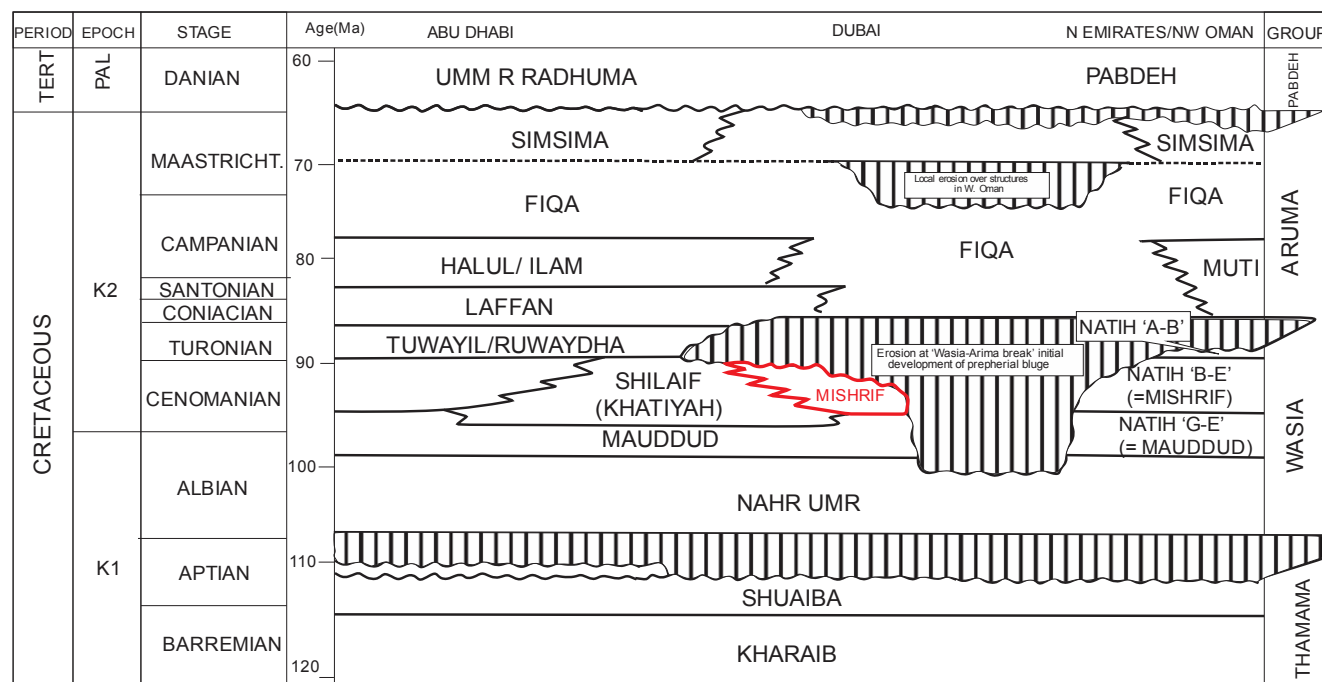


FIGURE 1. Chronostratigraphic chart of the mid-Cretaceous in the South Persian Gulf and Oman (Haq *et al.*, 1988).

The Sirri region in the Persian Gulf is hosting several oil fields (including A, B and C fields) (Fig. 2) that encompasses an extensive sedimentary basin situated between the Qatar Arc in the West, the Zagros area in the North, the Oman in the South-East, and extended southwards to Rub-Alkhali desert (Bashari and Minaei, 2003). Well A is located on an anticline structure with NNE-SSW axis, and wells B and C have been drilled on dome structures seemingly resulted from Cambrian salt diapirs.

DATA SET AND METHODS

In this study, to investigate and identify the heterogeneities of the Mishrif reservoirs in the Sirri Oil fields, data from three wells A, B and C (one well from each field) were used (Fig. 2). This study was based on the logging of drill-cores and slabs (total thickness of 202m), 246 semi-stained thin sections and 800CCAL poroperm data associated with petrophysical well logs from the mid-Cenomanian Mishrif Fm. which was obtained from three exploration/appraisal wells (A, B and C) of the Sirri Oil fields.

To investigate depositional facies distribution and diagenetic features, petrographic analyses (microfacies analysis and diagenetic studies on thin sections) were performed. Geochemical data for detailed analysis of depositional and diagenetic characteristics were not available. Facies analysis was carried out using standard models and microfacies descriptions (*e.g.* Wilson, 1975; Flügel, 2010). Detailed petrographic studies for facies analysis and determination of diagenetic factors controlling the distribution of reservoir (flow units) and non-reservoir (barrier/baffle) units in the Mishrif Fm. was done. In this respect, semi-quantitative inspection of carbonate components, using the comparative charts suitable for visual estimation in carbonate rocks (Baccelle

and Bosellini, 1965), was made. For facies classification, scheme suggested by Embry and Klovan (1971), is considered. To define controlling factors for reservoir quality results from depositional facies analysis, and reconstruction of their diagenetic history within a sequence stratigraphic framework, are integrated. The sequence stratigraphic framework of the Mishrif reservoir intervals is considered as the basis for a geological-based reservoir zonation. To construct such a framework and define the main sequence surfaces -Sequence Boundaries (SBs) and Maximum Flooding Surfaces (MFSs)-, several data were used. They include results of facies analysis and wireline logs (especially gamma-ray and bulk density). To determine the sequence boundaries, rapid changes in facies and distinct diagenetic overprints related to relative sea-level falls were considered. Then, flow units were determined based on FZI (Amaefule *et al.*, 1993; Abbaszadeh *et al.*, 1996) and water saturation was calculated by Archie equation (Archie, 1942)(4) and electrical resistivity log. Finally, the results from geological (facies, diagenesis and sequence stratigraphy interpretation) and petrophysical studies were integrated for the description of reservoir zones and determination of hydrocarbon column in the Sirri Oil fields.

DEPOSITIONAL CHARACTERISTICS

For facies analysis, several parameters including allochemical components (skeletal and non-skeletal), sedimentary textures, micrite content, bulk mineralogy or lithology and depositional features were investigated in detail. These led to the identification of eight facies formed in seven facies belts in the studied formation in three fields A, B and C. Depositional, diagenetic and reservoir properties (porosity and permeability) of these facies have been summarized in Table 1. Comparison of the facies, based on their texture, fossil content and facies association, with

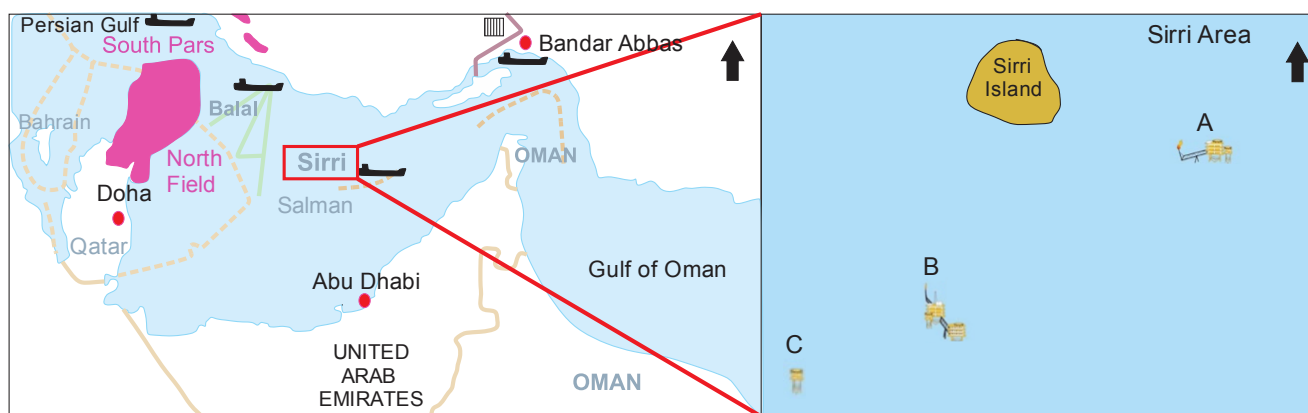


FIGURE 2. Location map of the studied fields (A, B and C) in the Persian Gulf.

standard facies belts of Flügel (2010), depicts a homoclinal carbonate ramp for their deposition and development. Accordingly, RMF1 (peloidal/bioclastic packstone to grainstone), RMF2 (large benthic foraminifera wackestone with rudist debris) and RMF3 (rudist debris floatstone) are attributed to inner ramp environment (Fig. IIA–F). RMF4 (rudist rudstone) and RMF5 (peloid bioclasts packstone/wackestone) deposited in mid-ramp (Fig. IIG–J). RMF6 (peloid bioclasts wackestone/mudstone) and RMF7 (mudstone) are related to outer ramp (Fig. IIK–N). Finally, RMF8 (planktonic foraminifera wackestone/mudstone) deposited in the basin realm (Fig. IIO, P). Most facies of the Mishrif Fm. in the studied fields are characterized by high-values of core porosity and permeability.

In well A, all identified facies (except RMF5 and RMF6) are present. However, in well B, just RMF3, RMF5 and RMF6 were recognized. In addition, in well C, RMF5, RMF6 and RMF7 are observed (Figs. 3; III). General facies distribution and facies belts are illustrated in a conceptual model of the carbonate ramp for the Mishrif Fm. in the Sirri Oil fields (Fig. 3). Comparing the facies associations frequency of the Mishrif Fm. in the studied fields, a general westward deepening in the depositional environment could be envisaged (from well A towards wells B and C) (Figs. III; IV; 4). This suggestion is approximately consistent with the paleogeographic map (Fig. 5) illustrating the distribution of Mishrif-Khatiya in the eastern Persian Gulf and North of Emirate (Rezaee, 2002). It is despite some inconsistencies (i.e. absence of RMF7 and RMF8 in well B and absence of RMF8 in well C), seemingly caused

by an erosional event occurred during the Cenomanian–Turonian subaerial exposure. This resulted in the removal of some shallow marine facies in some areas as observed in the structural position of well C (on the top of an anticline) and so these facies are not observed in this well. Sedimentological logs depicted for each well, indicates a shallowing upward trend of facies in response to a relative sea-level change during mid-Cretaceous.

Huge volumes of rudist debris (ranging from gravel to silt in size) originated from initial rudist community, gathered as bioclastic shoals and talus deposits on many Cretaceous carbonate platforms of the Middle East (Esrafil-Dizaji *et al.*, 2015). Rudist debris occur in most studied microfacies with various shapes and sizes. Generally, rudist-dominated units of the Mishrif Fm. are known as the “Rudist debris zone” in the biozonation scheme of the Zagros area (Wynd, 1965; Omidvar *et al.*, 2014). Seemingly, these units could be correlated with the same rudist-dominated intervals of the Mishrif Fm. in the Persian Gulf, Iraq, and the United Arab Emirates and of the Natih Fm. of Oman (Alsharhan, 1995; Van Buchem *et al.*, 1996; Mahdi and Aqrabi, 2014; Sadooni, 2005). Generally, the rudist-dominated facies were subjected to fresh water diagenesis during a relative sea-level fall. Where they were subaerially exposed their initial porosity was enhanced by extensive meteoric dissolution. Of course, away from the subaerial exposure surfaces, same facies show poor-quality reservoir. In this situation, the porosity is reduced by meteoric and shallow to deep burial cements, and mechanical/chemical compaction. Despite their depth of

TABLE 1. Sedimentary and diagenetic characteristics of the identified microfacies in the studied fields

| Well | Dominant diagenetic features | Mean K (mD) | Mean PHI (%) | RAMF (Flügel) | Facies Belt | Components | | Microfacies | Facies code |
|------|---|-------------|--------------|---------------|--------------------------------------|-----------------|---|--|-------------|
| | | | | | | Non Skeletal | Skeletal | | |
| A | Physical compaction, micritization, dissolution | 6.7 | 19 | 26 | Inner ramp-shoal | Peloid, Cortoid | Bioclasts, rudist debris | Peloidal/bioclastic packstone to grainstone | RMF1 |
| A | Micritization, dissolution, neomorphism, pyritization | 7.96 | 15.35 | 13 | Inner ramp-restricted open marine | Peloid | Large benthic foram, rudist debris, bioclasts | Large benthic foraminifera wackestone with rudist debris | RMF2 |
| A, B | Physical compaction, micritization, dissolution, cementation | 34.26 | 22.76 | 15 | Inner ramp-restricted open marine | Peloid | Rudist debris, benthic foram, bioclasts | Rudist debris floatstone | RMF3 |
| A | Physical compaction, micritization, dissolution, cementation (low) | 21.06 | 16.81 | 12 | Mid ramp-reef talus | Peloid, Cortoid | Rudist debris, bioclasts | Rudist rudstone | RMF4 |
| B, C | Physical compaction, micritization, dissolution, cementation (low) | 69.43 | 23.93 | 4 | Mid ramp-middle part to end part | Peloid | Rudist debris, bioclasts, echinoids | Peloidbioclast packstone/wackestone | RMF5 |
| B, C | Micritization, chemical compaction, fracturing, cementation | 19.42 | 23.53 | 2 | Outer ramp-first part to middle part | Peloid | Rudist debris, bioclasts, echinoids | Peloidbioclast wackestone/mudstone | RMF6 |
| A, C | Chemical compaction, fracturing, cementation, burial dissolution, neomorphism | 13.26 | 19.54 | 2 | Outer ramp-end part | - | Echinoids | Mudstone | RMF7 |
| A | Chemical compaction | 3.12 | 1.97 | 5 | Basin | - | Bioclasts, planktonic foram | Planktonic foraminifera wackestone/mudstone | RMF8 |

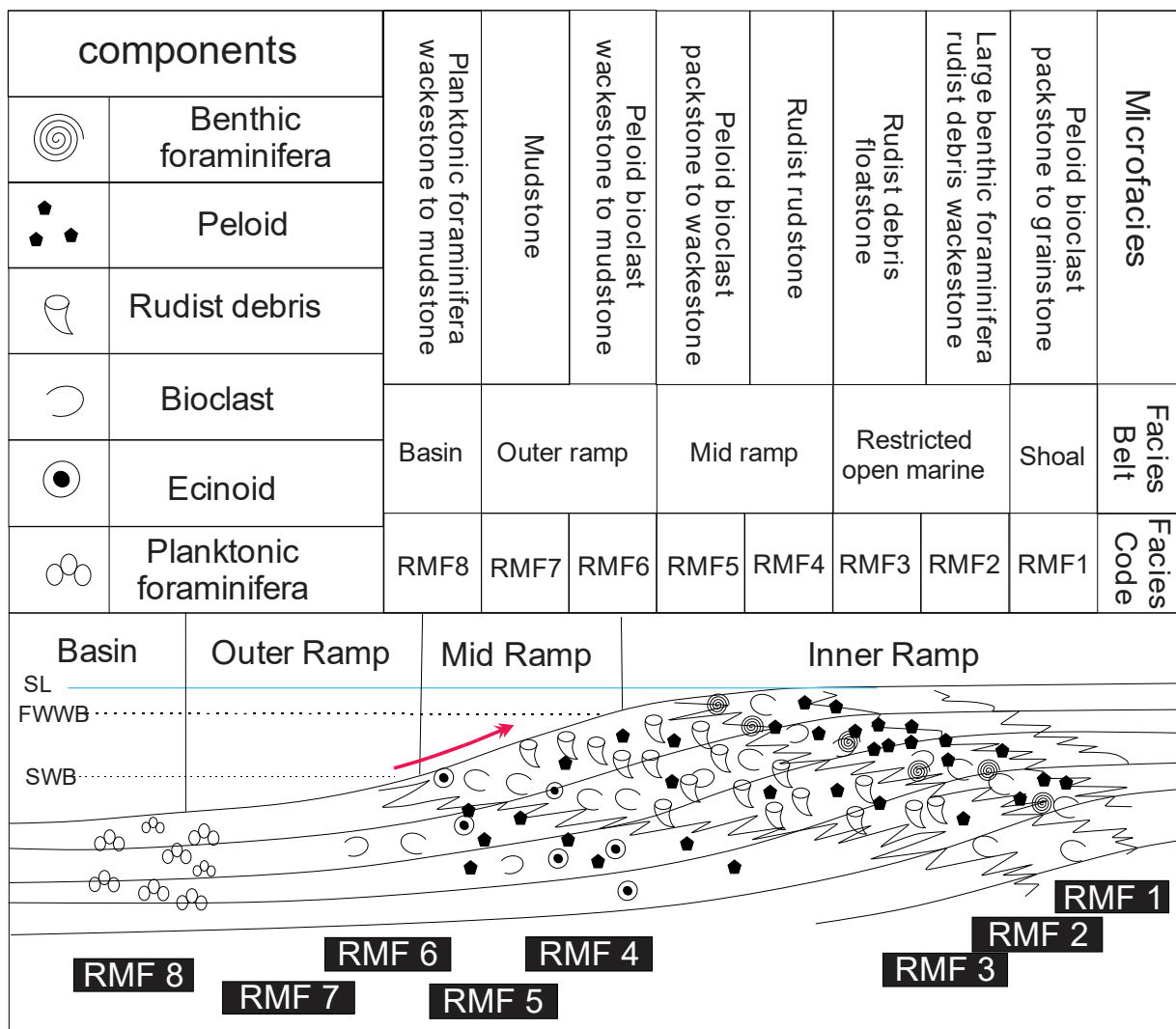


FIGURE 3. Depositional model (homoclinal ramp) for the Mishrif Fm. in the Sirri Oil field showing the distribution of microfacies and facies belts in different parts of the model. The arrow on this model indicates the shallowing upward trend of facies.

burial, significant amounts of porosity (>10%) are still preserved in the rudist-dominated facies of the Mishrif Fm., especially below disconformity surfaces.

DIAGENETIC PROCESSES AND FEATURES

Diagenetic processes are among the most important factors affecting the quality of carbonate reservoirs and impart important role on the distribution of reservoir parameters such as porosity and permeability (Schlager, 2005). In the case of Albian–Turonian Mishrif interval in the Arabian Plate, diagenesis has great contribution in controlling the reservoir characteristics (Hollis, 2011). During the Mishrif deposition in the studied area, due to the humid climate condition and relative sea-level fluctuation, the carbonate sediments were subaerially

exposed and endured significant modification in their initial sedimentary characteristics. In this study, diagenetic processes are described as follows.

Marine diagenetic processes

Micritization and bioturbation are dominant diagenetic processes related to stagnant marine phreatic environment in the studied wells. In addition, very fine and thin isopachous microcrystalline calcite cement, probably formed as an active marine phreatic cement, is rarely observed in some facies (Fig. V).

Meteoric diagenetic processes

Meteoric dissolution is the most important and widespread diagenetic processes in the Mishrif reservoir.

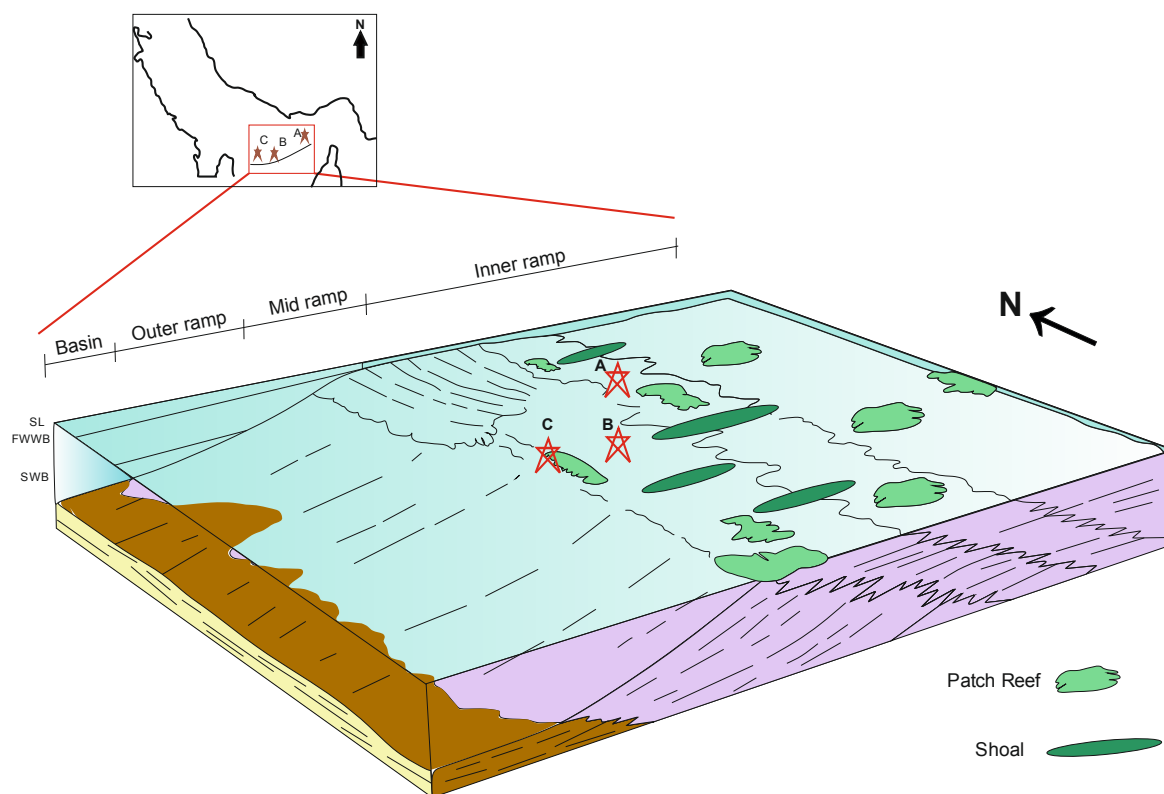


FIGURE 4. Approximate situation of the studied wells on a homoclinal ramp model of the Mishrif-Khatiya based on the frequency of identified carbonate facies.

It is characterized by nonselective grain and matrix dissolution, development of connected and non-connected vugs and karstification, especially around the sequence boundaries (Fig. VIA, B). Neomorphism is another feature of the meteoric diagenesis in the studied wells that occurred as aragonite and high-Mg calcite components inversion to low-Mg calcite (Fig. VIC) and matrix recrystallization (Fig. VID). Isopachous and blocky calcite cements, with a clear appearance and relatively coarse crystals are considered as the meteoric origin (Fig. VIE). In addition, geopetal fabric is attributed to the meteoric environment (Fig. VIF).

Burial diagenetic processes

Shallow burial diagenetic processes in the Mishrif are recognized by physical compaction (*e.g.* deformation of fossils components, compacted fabric and fracturing) (Fig. VIIA, B). In deeper burial environment, diagenetic processes are chemical compaction (solution seams and stylolite), burial cementation and dissolution, fracturing, dolomitization and pyritization (Fig. VIIC–L).

Extensive cementation in the Mishrif, especially in well A, is identified by equant, drusy and coarse crystalline calcite cements. Sometimes, they appear as fractures and vugs fillings. Considering the fact that a

significant part of these cements has been developed after the compaction and precipitation of primary cements (marine and meteoric), and they show sharp cleavages, sometimes even undulose extensions suggesting deeper burial origin (Fig. VIID, E). Burial dissolution in the Mishrif Fm., which has been previously reported by other workers (*e.g.* Mazzullo and Harris, 1991, 1992; Ehrenberg *et al.*, 2012), occurred as dissolution on burial cements and along stylolite (Fig. VIIC, L). Fracturing that observed as both filled and open fractures is mainly attributed to the burial realm (Fig. VIIC, K).

Dolomitization in the Mishrif Fm. has been mostly developed as replacement along the stylolites, and also sparse crystals within the matrix. Stylolite-related dolomites are fine to medium in size with euhedral to subhedral crystals (Fig. VIIF). Sparse, very fine to medium in size and euhedral to subhedral dolomite crystals is observed in mud-dominated facies (Fig. VIIG). Pyritization is the secondary in origin and is characterized by replacement of shell fragments or burial calcite cements (Fig. VIIH, I). Depicted paragenetic sequences of diagenetic events in the Mishrif Fm. for the studied fields are shown in Figure 6. In addition, the sequences of observed diagenetic events in the Mishrif reservoir is illustrated in Figure 7.

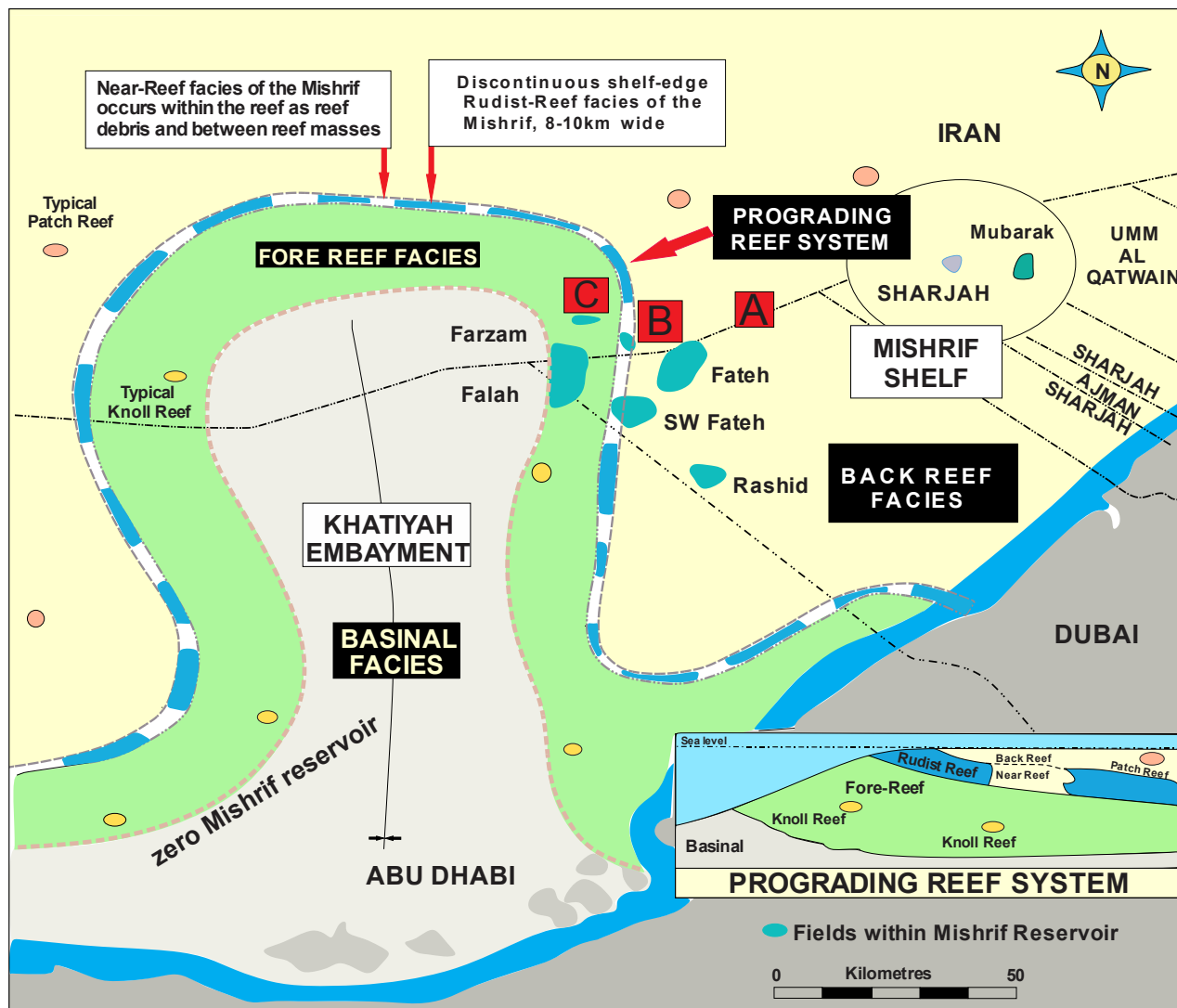


FIGURE 5. A schematic map illustrating development of the Khatiya Basin with marginal reefs (Mishrif) in the East of Persian Gulf, and the location of the studied fields (A, B and C) in this basin (Rezaee, 2002).

SEQUENCE STRATIGRAPHY

In this study, the sequence stratigraphic analysis for the Mishrif Fm. has been accomplished based on the T–R method (Embry and Johannesen, 1992) that was used as a basis for reservoir zonation and stratigraphic correlation. The sequence boundaries have been identified by changes in the trend of depositional environment and diagenetic features related to the relative sea-level fall and correlation of the results, where possible, with the gamma-ray and density log responses. Based on this technique, in well A, a Regressive System Tract (RST) (hemi-sequence) below the mid-Cenomanian unconformity and a third order sequence from the mid-Cenomanian boundary to Cenomanian–Turonian boundary were identified. In well B, only a third order sequence within the Mishrif interval is recognized, which is located just below the Cenomanian–

Turonian boundary. Also, in well C, only one RST below the Cenomanian–Turonian boundary was defined (Fig. 7; Table 2). In the studied fields, no evidences for mid-Turonian unconformity are observed, and regarding that the Mishrif is overlain by the Coniacian shaly Laffan Fm., a non-depositional event and time gap is suggested for the Turonian. The identified sequences in the studied fields are well-correlated with the sequence stratigraphic framework proposed for the other areas in the Persian Gulf and Arabian Plate (*e.g.* Van Buchem *et al.*, 1996, 2011).

HYDRAULIC FLOW UNITS AND RESERVOIR ZONATION

Porosity and permeability are considered as two main factors for investigation of the reservoir quality. As showed in Table 1, the Mishrif Fm. in the studied fields consists

TABLE 2. Sedimentary and diagenetic properties of the identified sequences in the studied wells

| WELL | System Tracts | Microfacies (From base to top of system track) | Diagenetic features |
|--------|---------------|---|--|
| WELL A | C-T-B | | |
| | RST | Wackestone with large benthic foraminifera and rudist debris - rudist debris floatstone related to restricted open marine in inner ramp | Dissolution vugs and moldic porosity and filled fractures |
| | TST | Floatstone with rudist debris (restricted open marine facies) - Rudist rudstone (first part of mid ramp) | Marine and meteoric calcite cementation-pyritization |
| WELL B | Mid-C-B | | |
| | RST | Microfacies of outer ramp - mid ramp - inner ramp (shoal facies) | Dissolution vugs and moldic porosity filled by burial calcite cement |
| WELL B | C-T-B | | |
| | RST | Bioclastic peloidal wackestone (mid ramp facies)- peloid bioclastic packstone to grainstone(shoal facies) | Extensive dissolution vugs and moldic porosity |
| WELL C | TST | Microfacies of mid ramp – outer ramp facies (deepening upward sequence) | pyritization |
| | C-T-B | | |
| WELL C | RST | Microfacies of outer ramp - mid ramp facies (middle part to end part) | Dissolution vugs in matrix |

of high-quality reservoir facies. Pore system properties, which have important effect on the fluid flow within a reservoir, are basically controlled by both the depositional and diagenetic characteristics. Carbonate reservoirs, in contrast to the clastic ones, show higher heterogeneity in pore throat properties of their pore system. Therefore, in most cases porosity and permeability distribution in these reservoirs do not show a clear correlation. Therefore, subdivision of the reservoir into units such as layers and horizons with their respected physical properties, support us in understanding the reservoir heterogeneity.

Hydraulic flow units are considered as a criterion for the reservoir units in which fluid flow properties is uniform due to the same pore throat properties (Kadkhodaie-Ilkhchi *et al.*, 2013). In other words, flow units based on the flow properties divide the reservoir into some certain zones that are useful for fluid simulation targets and reservoir layering (Bhattacharya *et al.*, 2008). Flow unit concept is used for differentiation of petrophysical rock types in the reservoir and each rock type has a certain value for FZI (Al-Ajmi and Holditch, 2000).

In this study, hydraulic flow units were determined based on FZI as proposed by Amaefule *et al.* (1993). A hydraulic flow unit is described as a part of the reservoir rock volume within which the pore throat properties of porous media controlling the fluid flow are consistent and predictably different from the other parts of the reservoir (Amaefule *et al.*, 1993; Abbaszadeh *et al.*, 1996; Porras and Campos, 2001). The steps for determination of the flow units are as follows:

First, Reservoir Quality Index (RQI) is calculated by using the method proposed by Amaefule *et al.* (1993):

$$RQI = 0.0314 \sqrt{K/\phi} \tag{1}$$

Where RQI: (μm); K: permeability (mD) and ϕ : porosity (in fraction).

The relationship between porosity and permeability with RQI for identified hydraulic flow units in the reservoir is shown in Figure VIII. Accordingly, the stronger relationship of the permeability with RQI implies the importance of pore throat properties in controlling of fluid flow in the reservoir.

Then, Pore to Matrix Ratio (PMR) is calculated as follows:

$$PMR = \left(\frac{\phi e}{(1-\phi)} \right) \tag{2}$$

Finally, FZI is determined by the following equation:

$$FZI = \frac{RQI}{PMR} \tag{3}$$

A plot of FZI values *versus* sample numbers shows the distribution of this parameter, which based on different flow units, can be differentiated and sorted (Fig. 8). This means

| Stage | Diagenesis | | | | |
|----------------|----------------------------|----------|---------|--------|------|
| Time | mid Cenomanian | | | Recent | |
| Environment | Marine and syndepositional | Meteoric | Shallow | Burial | Deep |
| Events | | | | | |
| Micritization | _____ | | | | |
| Compaction | | | _____ | | |
| Cementation | | _____ | | | |
| Dissolution | | _____ | | | |
| Neomorphism | | | | | |
| Dolomitization | | | | _____ | |
| Pyritization | | | | _____ | |
| Fracturing | | | | | |

FIGURE 6. Paragenetic sequence of diagenetic processes illustrated for the Mishrif Fm. in the studied fields.

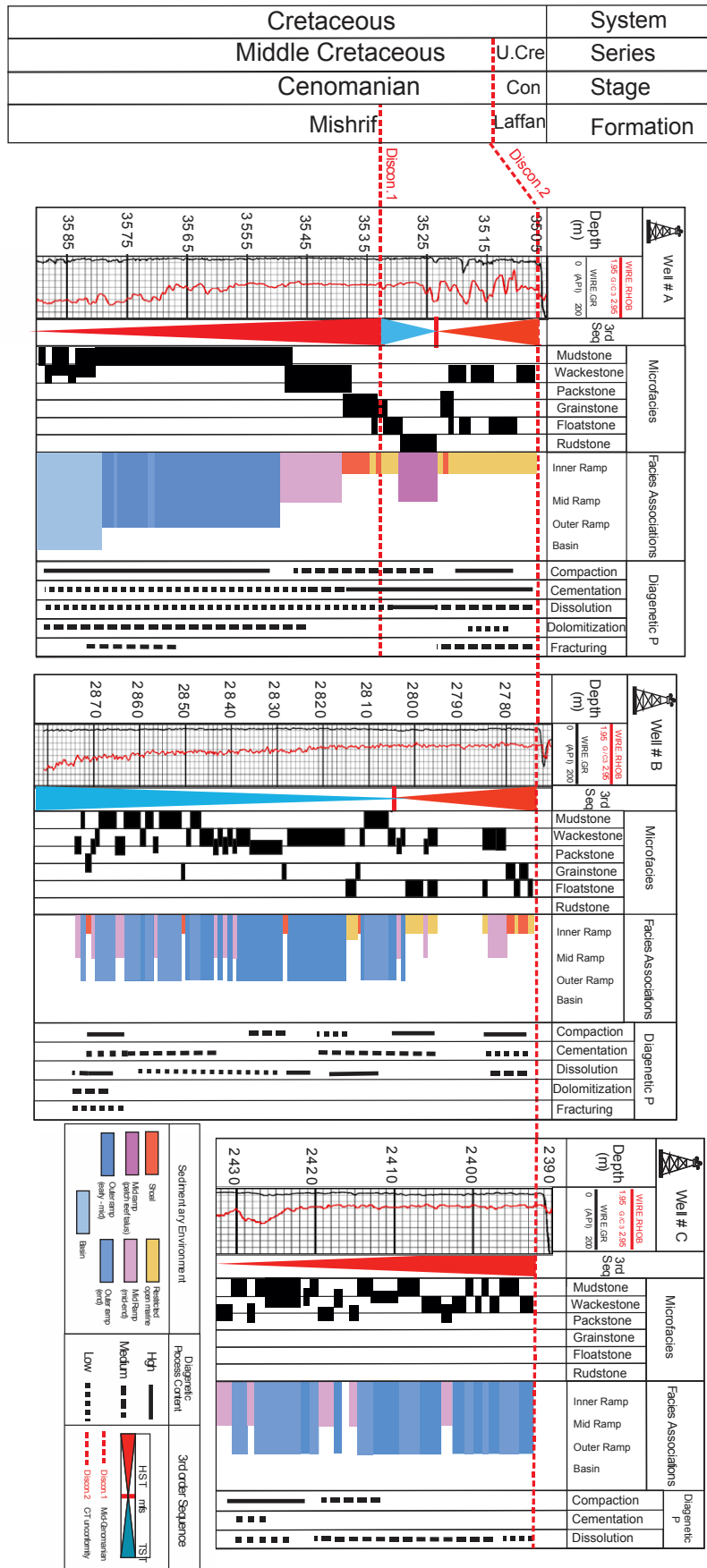


FIGURE 7. Correlation of the third order sequences in wells A, B and C in Sirri Oil fields. The sequences and sequence boundaries were identified by the facies characteristics, diagenetic features and variations in well log responses. The time scale for sequences and sequence boundaries have been determined by comparison with the equivalent intervals in the adjacent fields and Arabian Platform. Biostratigraphic data were not available.

samples with similar values of FZI belong to a specific flow unit. Based on this method, four HFUs (A, B, C and D) in the Mishrif reservoir were identified which on the basis of their capability for the fluid flow can be classified into four main rock types with very high- (HFUD), high- (HFUC), medium- (HFUB) and low- (HFUA) quality (Table 3). Investigation of identified hydraulic flow units on porosity and permeability plot (Fig. IX) shows that each HFU is characterized by a certain district on the plot. This property is attributed to pore system properties controlling the fluid flow in the reservoir.

To reach an insight from the factors controlling the pore system properties in each flow unit, depositional and diagenetic characteristics of their related facies were investigated. The results indicate a close relationship between the sedimentary/ diagenetic properties of facies and their petrophysical properties. As, HFUA with high-porosity and low-permeability is mainly related to mud-dominated and grain-dominated facies of the mid ramp and outset of the outer ramp with non-touching vugs and moldic pores mostly resulted from meteoric dissolution (Fig. XA, B). HFUB and HFUC as intermediate flow units, include lagoon, talus and shoal facies which have been affected by meteoric dissolution and cementation. Most of the pore spaces in these facies are touching vugs (Fig. XC–F). The HFUB and HFUC just differ in the amount of the porosity and permeability. HFUD with high-quality involves facies of the open marine lagoon and middle part of mid-ramp to outer ramp with touching and separate micro vugs. Due to the presence of open and enlarged fractures in this facies, they show high-permeability, despite low-porosity (Fig. XG, H). The important feature of this HFU is the role of fracturing and the burial dissolution on the permeability enhancement. Depositional and diagenetic characteristics of identified flow units are summarized in Table 4.

The frequency distribution of different hydraulic flow units in three studied wells, as shown in Figure XI, demonstrates that a significant part (about 80%) of the Mishrif reservoir is composed of medium- to high-quality flow units. Generally, due to the higher average porosity and permeability of the Mishrif interval in the Sirri fields, it can be considered as a reservoir zone with high storage capacity and fluid conductivity. General flow units' distributions within the sequence stratigraphic framework of the field and associated sedimentary/diagenetic characteristics, are shown in Figure 9.

HYDROCARBON COLUMN

Since the main objective of the reservoir heterogeneity assessment and evaluation is the hydrocarbon

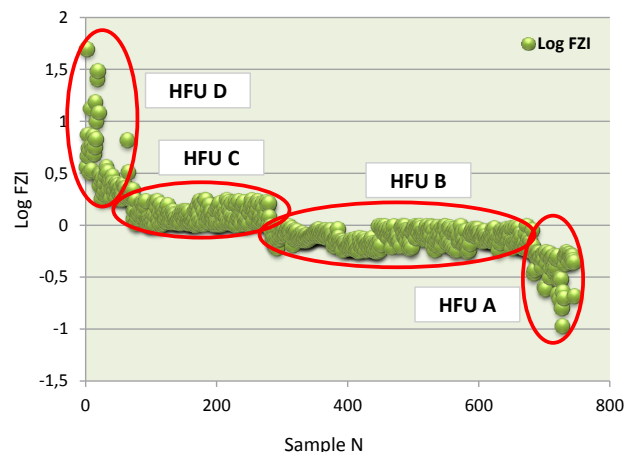


FIGURE 8. Log Flow Zone Indicator (FZI) versus sample numbers for determination of hydraulic flow units in the reservoir.

exploration, it is important to identify the porous and permeable reservoir zones with low water saturation and high volumes of hydrocarbon. So, in order to calculate the water saturation and to investigate distribution of hydrocarbon bearing zones within the reservoir interval, Archie equation (Archie, 1942) (4) and resistivity logs (equivalent resistivity log, LLD) were used in the studied wells. In this equation, LLD is used as true formation resistivity (RT).

$$F = \left(\frac{a}{\phi^m} \right) \quad SW = \sqrt[n]{\left(\frac{a}{\phi^m} \right) \times \left(\frac{R_w}{R_t} \right)} \quad (4)$$

Where F: Formation resistivity factor; a: tortuosity; m: cementation factor; n: saturation factor.

With regard to a carbonate lithology for the reservoir, Archie's parameters a, m and n are set to default as follows:

$$a: 1 \quad m: 2 \quad n: 2$$

Formation Water Resistivity (Rw) according to the well log headers is 0.02Ωm and porosity is equivalent to neutron log.

Then, water saturation log for the Mishrif reservoir interval in the studied wells was prepared (Fig. 9). The results show that in well A, despite the high-thickness

TABLE 3. Cut off values based on Flow Zone Indicator (FZI) for differentiation of HFUs in the reservoir, associated with reservoir quality index and average porosity and permeability data

| HFU | Porosity (%) | Permeability (mD) | Cut off Value | Reservoir quality |
|-----|--------------|-------------------|----------------------|-------------------|
| A | 18.79 | 2.98 | Log FZI < -0.25 | Low |
| B | 22.19 | 14.4 | - 0.25 < Log FZI < 0 | Medium |
| C | 18.98 | 24.21 | 0 < Log FZI < 0.25 | High |
| D | 14.02 | 61.13 | Log FZI > 0.25 | Very high |

TABLE 4. The identified hydraulic flow units in relation to their depositional and diagenetic characteristics

| HFUs | Microfacies | Diagenetic Features | Mean PHI (%) | Mean K (mD) | FZI cut off and Reservoir quality class |
|------|-------------------------------------|--|--------------|-------------|---|
| HFUA | RMF5, RMF6 | Physical and chemical compaction; Burial dolomitization; Moldic porosity (in grain dominated facies); Separate vugs and microporosity in mud- dominated facies; filled fractures | 18.79 | 2.98 | Log FZI < -0.25 Low reservoir quality |
| HFUB | RMF1, RMF2, RMF3, RMF4, RMF5, RMF6, | High Meteoric dissolution; Physical compaction; meteoric cement; touching vugs porosity (in micrite) | 22.19 | 14.4 | -0.25 < Log FZI < 0 Medium reservoir quality |
| HFUC | RMF1, RMF2, RMF3, RMF4, RMF5, RMF6, | High meteoric dissolution; physical compaction; low meteoric cement; touching vug porosity (in micrite) | 18.98 | 24.21 | 0 < Log FZI < 0.25 High reservoir quality |
| HFUD | RMF2, RMF3, RMF4, RMF6 | Physical and chemical compaction; open fracture; burial dissolution; vug porosity (touching and separate) | 18.98 | 61.13 | Log FZI > 0.25 Very high reservoir quality |

of the reservoir zone according to flow units, only about half of this thickness (with present water saturation), can be considered as hydrocarbon bearing zone. Also, in well B, 8.5m from the total reservoir zone (91m) is accounted for the hydrocarbon zone, and most of the reservoir due to the high water saturation is full of water. In well C, in comparison with the other wells, almost the total of the reservoir zone is compatible with the hydrocarbon zone. Finally, in order to reach a general view of the hydrocarbon zone and its thickness variations in the studied fields, this zone was correlated between the wells (Fig. 9). According to this correlation, there is a decrease in thickness of hydrocarbon zone from well A towards well B, but from well B towards well C, the thickness is increased, as the total of Mishrif interval in well C change to a hydrocarbon zone.

In addition, hydrocarbon zone in three studied wells can be correlated with Cenomanian–Turonian and mid-Cenomanian sequence boundaries (Fig. 9). Variation in the thickness of hydrocarbon zone in these wells is attributed to different position of the wells on the related structures with a tilted (northward) oil-water contact (Fig. 10). Well A has been drilled on the deeper part and flank of the structure, while well B is located near the top and well C is drilled just on the top of the structure. Well C, which has been drilled on the eroded top of the structure (Cenomanian–Turonian unconformity), includes a high-thickness of hydrocarbon column. Low-thickness of hydrocarbon zone in well B can be related to tilted oil-water contact with a slope to the North (Rezaee, 2002).

CONCLUSIONS

Petrographic analysis of the Mishrif Fm. in the studied fields showed that different facies have been deposited in the inner to outer parts of a homoclinal carbonate ramp. Variations in distribution and frequency of different facies in the studied wells is mainly related to their position on the platform. Humid climate condition and tectonic activity in association with eustatic sea-level fluctuations during the mid-Cretaceous, led to extensive meteoric diagenesis of Mishrif carbonates through subaerial exposure. In well A, evidences for two subaerial exposures within the Mishrif interval are recognized, whereas in wells B and C only one exposure event is distinguished. In addition, investigation of the diagenetic history of the Mishrif Fm. in studied fields indicates complex history of the diagenetic events related to eogenetic, mesogenetic and telogenetic realms. These diagenetic processes exerted important control over the reservoir zones development within the formation. Thus, meteoric dissolution enhanced the reservoir quality and is mainly related to the periods of subaerial exposure on the disconformity surfaces. On the other hand, cementation had negative effects on the reservoir quality.

The sequence stratigraphic analysis based on T–R method, and use of the integrated results from facies and diagenetic studies led to identification of a third order sequence and a hemi-sequence (RST) in well A with two unconformity surfaces (mid-Cenomanian and Cenomanian–Turonian), a third order sequence with Cenomanian–Turonian unconformity in well B, and

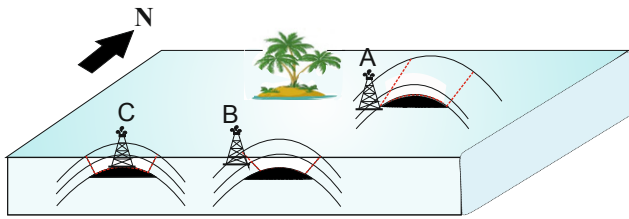


FIGURE 10. A schematic showing the location of the studied wells on the structure in the Sirri fields of the Persian Gulf.

a hemi-sequence (RST) with Cenomanian–Turonian unconformity in well C.

HFUs were determined based on FZI method and so four flow units (A, B, C and D) were recognized. Their reservoir quality increases from HFU A to D. The results showed that a significant part of the Mishrif carbonates in three studied wells, due to their complex sedimentary and diagenetic history, show high-quality reservoir. Therefore, it can be concluded that both the sedimentary and diagenetic processes controlled the HFUs distribution in the Mishrif reservoir.

Calculation of water saturation within the reservoir indicates that the thickness of hydrocarbon bearing zone in the studied wells is different. This difference is attributed to different location of the wells on the platform structures and tilted (northward) oil-water contact. The location of the hydrocarbon zone in the studied wells is related to the Cenomanian–Turonian and mid-Cenomanian sequence boundaries. In the studied wells, there is no significant difference in the diagenetic imprints above and below oil-water contact.

ACKNOWLEDGMENTS

The University of Tehran is thanked for providing facilities for this research. The authors acknowledge Iranian Offshore Oil Company for sponsorship and data preparation.

REFERENCES

- Abbaszadeh, M., Fujii, H., Fujimoto, F., 1996. Permeability prediction by hydraulic flow unit's theory and applications. Society of Petroleum Engineers (SPE) Formation Evaluation, 11(4), 263-271.
- Ahr, W.M., 2008. Geology of carbonate reservoirs. Chichester, John Wiley and Sons, 296pp.
- Al-Ajmi, F.A., Holditch, S.A., 2000. Permeability estimation using hydraulic flow units in a central Arabia reservoir. Dallas (Texas, USA), Society of Petroleum Engineers (SPE), Annual Technical Conference and Exhibition, 1-4 October.

- Al-Habashi, A., Darwish, A.R., Hamdy, T., Shebl, H., 2003. Application Of Sequence Stratigraphy And Petrography In Preparation Of Reservoir Rock Typing Scheme In One Of Thamama Gas Reservoirs Of Onshore Abu Dhabi. In Middle East Oil Show. Society of Petroleum Engineers (SPE), Middle East Oil Show, 11pp. DOI: 10.2118/81533-MS
- Al-Khersan, H., 1975. Depositional environments and geological history of the Mishrif Formation in southern Iraq. Dubai, Proceeding at 4th Arab Petroleum Congress, 121(B-3), 1-18.
- Al-Mohammad, R.A.H., 2012. Depositional Environment and Petrophysical properties study of Mishrif Formation in Tuba Oilfield, Southern Iraq. Journal of Basrah Researches (Sciences), 38(1.A), 25-50.
- Alsharhan, A., 1995. Facies variation, diagenesis and exploration potential of the Cretaceous rudist bearing carbonates of the Persian Gulf. American Association of Petroleum Geologists Bulletin, 79(4), 531-550.
- Alsharhan, A.S., Nairn, A.E.M., 1986. A review of the Cretaceous formations in the Arabian Peninsula and Gulf: Part I. Lower Cretaceous (Thamama Group), stratigraphy and paleogeography. Journal of Petroleum Geology, 9(4), 365-392.
- Alsharhan, A.S., Nairn, A.E.M., 1988. A review of the Cretaceous formations in the Arabian Peninsula and Gulf: Part II, mid-Cretaceous (Wasia Group), stratigraphy and paleontology. Journal of Petroleum Geology, 11(1), 89-112.
- Alsharhan, A.S., Kendall, C.G.St.C., 1991. Cretaceous chronostratigraphy, unconformities and eustatic sea level changes in the sediments of Abu Dhabi, United Arab Emirates. Cretaceous Research, 12(4), 379-401.
- Amæfule, J.O., Altunbay, M., Tiab, D., Kersey, D.G., Keelan, D.K., 1993. Enhanced reservoir description: using core and log data to identify hydraulic (flow) units and predict permeability in uncored intervals/wells. Society of Petroleum Engineers (SPE), Annual Technical Conference and Exhibition, 16pp. DOI: 10.2118/26436-MS
- Aqrabi, A.A.M., Thehni, G.A., Sherwani, G.H., Kareem, B.M.A., 1998. Mid-Cretaceous rudist bearing carbonates of the Mishrif formation: an important reservoir sequence in the Mesopotamian basin, Iraq. Journal of Petroleum Geology, 21(1), 57-82.
- Aqrabi, A.A.M., Mahdi, T.A., Sherwani, G.H., Horbury, A.D., 2010. Characterisation of the Mid-Cretaceous Mishrif Reservoir of the Southern Mesopotamian Basin, Iraq. Bahrain, In American Association of Petroleum Geologists, GEO Middle East Geoscience Conference and Exhibition, March 7-10.
- Archie, G.E., 1942. The electrical resistivity log as an aid in determining some reservoir characteristics. Society of Petroleum Engineers (SPE), Transactions of the AIME, 146(01), 54-62.
- Assadi, A., Honarmand, J., Moallemi, S.A., Abdollahie-Fard, I., 2016. Depositional environments and sequence stratigraphy of the Sarvak Formation in an oil field in the Abadan Plain, SW Iran. Facies, 62, 26. DOI: 10.1007/s10347-016-0477-5

- Baccelle, L., Bosellini, A., 1965. Diagrammi per la stima visiva: della composizione percentuale nelle rocce sedimentarie. *Annali dell'Università di Ferrara*, 9(4), 59-62.
- Bashari, A., Minaei, M., 2003. Regional study of Mishrif and Ilam formations in the Sirri district of the Persian Gulf. Barcelona (Spain), American Association of Petroleum Geologists International Conference and Exhibition Technical Program, September 21-24.
- Bhattacharya, S., Byrnes, A.P., Watney, W.L., Doveton, J. H., 2008. Flow unit modeling and fine-scale predicted permeability validation in Atokan sandstones: Norcan East field, Kansas. *American Association of Petroleum Geologists Bulletin*, 92(6), 709-732.
- Blanc, E.J.-P., Allen, M.B., Inger, S. Hassani, H., 2003. Structural styles in the Zagros simple folded zone, Iran. *Journal of Geological Society*, 160(3), 401-412.
- Burchette, T.P., 1993. Mishrif Formation (Cenomanian-Turonian), Southern Arabian Gulf: Carbonate platform growth along a cratonic basin margin. In: Simo, J.A., Scott, R.W., Masse, J.-P. (eds.). *Cretaceous Carbonate Platforms*. American Association of Petroleum Geologists Memoir, 56, 185-199.
- Burchette, T.P., Britton, S.R., 1985. Carbonate facies analysis in the exploration for hydrocarbon: A case-study from the Cretaceous of Middle East. *Geological Society of London*, 18 (Special Publications), 311-338. DOI: 10.1144/GSL.SP.1985.018.01.13
- Davies, R.B., Casey D.M., Horbury A.D., Sharland, P.R., Simmons, M.D., 2002. Early to mid-Cretaceous mixed carbonate-clastic shelfal systems: examples, issues and models from the Arabian Plate. *GeoArabia*, 7(3), 541-598.
- Droste, H., Van Steenwinkel, M., 2004. Stratal geometries and patterns of platform carbonates: the Cretaceous of Oman. In: Eberli, G., Masferro, J.L., Sarg, J.F.R. (eds.). *Seismic Imaging of Carbonate Reservoirs and Systems*. American Association of Petroleum Geologists Memoir, 81, 185-206.
- Ehrenberg, S.N., Nadeau, P.H., Aqrawi, A.A.M., 2007. A comparison of Khuff and Arab reservoir potential throughout the Middle East. *American Association of Petroleum Geologists Bulletin*, 91(3), 275-286.
- Ehrenberg, S.N., Aqrawi, A.A., Nadeau, P.H., 2008. An overview of reservoir quality in producing Cretaceous strata of the Middle East. *Petroleum Geoscience*, 14(4), 307-318.
- Ehrenberg, S.N., Walderhaug, O., Bjorlykke, K., 2012. Carbonate porosity creation by mesogenetic dissolution: Reality or illusion? *American Association of Petroleum Geologists Bulletin*, 96(2), 217-233.
- Emami, H., Vergés, J., Nalpas, T., Gillespie, P., Sharp, I., Karpuz, R., Blanc, E.P., Goodarzi, M.G.H., 2010. Structure of the Mountain Front Flexure along the Anaran anticline in the Pusht-e Kuh Arc (NW Zagros, Iran): insights from sand box models. In: Leturmy, P., Robin, C. (eds.). *Tectonic and Stratigraphic Evolution of Zagros and Makran during the Meso-Cenozoic*. Geological Society of London, 330 (Special Publications), 155-178.
- Embry, A.F., Klovan, J.E., 1971. A late Devonian reef tract on north-eastern Banks Island, N.W.T. *Bulletin of Canadian Petroleum Geology*, 19(4), 730-781.
- Embry, A.F., Johannessen, E.P., 1992. T-R sequence stratigraphy, facies analysis and reservoir distribution in the uppermost Triassic-Lower Jurassic succession, western Sverdrup Basin, Arctic Canada. *Norwegian Petroleum Society*, 2 (Special Publications), 121-146.
- Esrifili-Dizaji, B., Rahimpour-Bonab, H., Mehrabi, H., Afshin, S., Harchegani, F.K., Shahverdi, N., 2015. Characterization of rudist-dominated units as potential reservoirs in the middle Cretaceous Mishrif Formation, SW Iran. *Facies*, 61:14. DOI: 10.1007/s10347-015-0442-8
- Flügel, E., 2010. Microfacies Analysis: Methods. In: Flügel, E. (ed.). *Microfacies of Carbonate Rocks*. Springer-Verlag Berlin Heidelberg, 53-72.
- Ghazban, F., Motiei, H., 2010. *Petroleum Geology of the Persian Gulf*. Tehran University Press, 707pp.
- Harris, P.M., Frost, S.H., Seiglie, G.A., Schneidermann, N., 1984. Regional unconformities and depositional cycles, Cretaceous of the Arabian Peninsula. In: Schlee, J.S. (ed.). *Interregional Unconformities and Hydrocarbon Accumulation*. American Association of Petroleum Geologists Memoir, 36, 67-80.
- Haq, B.U., Hardenbol, J., Vail, P.R., 1988. Mesozoic and Cenozoic chronostratigraphy and cycles of sea-level change. *American Association of Petroleum Geologists, Special publications of Society of Economic Paleontologists and Mineralogists*, 42, 71-108.
- Hollis, C., 2011. Diagenetic controls on reservoir properties of carbonate successions within the Albian-Turonian of the Arabian Plate. *Petroleum Geoscience*, 17(3), 223-241. DOI: 10.1144/1354-079310-032
- Jordan, C.F.Jr., Connolly, T.C.Jr., Vest, H.A., 1985. Middle Cretaceous Carbonates of the Mishrif Formation, Fateh Field, Offshore Dubai, U.A.E. In: Roehland, P.O., Choquette, P.W. (eds.). *Carbonate Petroleum Reservoirs*. New York, Springer-Berlag, 426-442.
- Kadhodaie-Ilkhchi, R., Rezaee, R., Moussavi-Harami, R., Kadhodaie-Ilkhchi, A., 2013. Analysis of the reservoir electrofacies in the framework of hydraulic flow units in the Whicher Range Field, Perth Basin, Western Australia. *Journal of Petroleum Science and Engineering*, 111, 106-120. DOI: 10.1016/j.petrol.2013.10.014
- Mahdi, T.A., Aqrawi, A.A.M., 2014. Sequence stratigraphic analysis of the mid-Cretaceous Mishrif Formation, southern Mesopotamian basin, Iraq. *Journal of Petroleum Geology*, 37(3), 287-312.
- Mazzullo, S.J., Harris, P.M., 1991. An overview of dissolution porosity development in the deep-burial environment, with examples from carbonate reservoirs in the Permian Basin. In: Candellaria, M.P. (ed.). *Permian Basin Plays*. Texas, Tomorrow's Technology Today: West Texas Geological Society Publication, 91-89, 125-138.
- Mazzullo, S.J., Chilingarian, G.V., 1992. Diagenesis and origin of porosity (Chapter 4). In: Chilingarian, G.V., Mazzullo, S.J.,

- Rieke, H.H. (eds.). Carbonate reservoir characterization: A geologic- engineering analysis, Part I. Amsterdam, Elsevier, 30, 199-270. DOI: 10.1016/S0376-7361(09)70127-X
- Mazzullo, S.J., Harris, P.M., 1992. Mesogenetic dissolution: Its role in porosity development in carbonate reservoirs. *American Association of Petroleum Geologists Bulletin*, 76(5), 607-620.
- Mehrabi, H., Rahimpour-Bonab, H., 2014. Paleoclimate and tectonic controls on the depositional and diagenetic history of the Cenomanian-early Turonian carbonate reservoirs, Dezful Embayment, SW Iran. *Facies*, 60(1), 147-167.
- Mehrabi, H., Rahimpour-Bonab, H., Hajikazemi, E., Jamalian, A., 2015. Controls on depositional facies in Upper Cretaceous carbonate reservoirs in the Zagros area and the Persian Gulf, Iran. *Facies*, 61(4), 1-24.
- McQuarrie, N., 2004. Crustal scale geometry of the Zagros fold-thrust belt, Iran. *Journal of Structural Geology*, 26, 519-535.
- Moore, C.H., 2001. Carbonate reservoirs: porosity evolution and diagenesis in a sequence stratigraphic framework. Amsterdam, The Netherlands, Elsevier Science, 460pp.
- Motiei, H., 1993. Stratigraphy of Zagros (In Persian). *Treatise on the Geology of Iran*, 60, 151pp.
- Omidvar, M., Mehrabi, H., Sajjadi, F., Bahramizadeh-Sajjadi, H., Rahimpour-Bonab, H., Ashrafzadeh, A., 2014. Revision of the foraminiferal biozonation scheme in Upper Cretaceous carbonates of the Dezful Embayment, Zagros, Iran: integrated palaeontological, sedimentological and geochemical investigation. *Revue de Micropaléontologie*, 57(3), 97-116. DOI: 10.1016/j.revmic.2014.04.002
- Petty, M.D., 2005. Paleoclimatic control on porosity occurrence in the Tilston interval, Madison group, Williston basin area. *American Association of Petroleum Geologists Bulletin*, 89(7), 897-919.
- Philip, J., Borgomano, J., Al-Maskiry, A., 1995. Cenomanian-Early Turonian carbonate platform of northern Oman: stratigraphy and palae-environments. *Paleogeography, Paleoclimatology, Paleoeology*, 119(1-2), 77-92.
- Porras, J.C., Campos, O., 2001. Rock typing: a key approach for petrophysical characterization and definition of flow units, Santa Barbara Field, Eastern Venezuela Basin. Society of Petroleum Engineers. Society of Petroleum Engineers (SPE), Buenos Aires (Argentina), Latin American and Caribbean Petroleum Engineering Conference, 25-28 March, 6pp.
- Rahimpour-Bonab, H., 2007. A procedure for appraisal of a hydrocarbon reservoir continuity and quantification of its heterogeneity. *Journal of Petroleum Science Engineering*, 58(1-2), 1-12.
- Rahimpour-Bonab, H., Esrafil-Dizaji, B., Tavaloli, V., 2009. Dolomitization and Anhydrite Precipitation in Permo-Triassic Carbonates at the South Pars Gasfield, Offshore Iran: Controls on Reservoir Quality. *Journal of Petroleum Geology*, 33(1), 43-66. DOI: 10.1111/j.1747-5457.2010.00463.x
- Razin, P., Taati, F., Van Buchem, F.S.P., 2010. Sequence stratigraphy of Cenomanian-Turonian carbonate platform margins (Sarvak Formation) in the High Zagros, SW Iran: An outcrop reference model for the Arabian Plate. *Geological Society of London*, 329(1, Special Publications), 187-218.
- Rezaee, J., 2002. Well completion report of well 1 of Farzam Field. Iranian Offshore Oil Company, 215pp.
- Sadooni, F.N., 2005. The nature and origin of Upper Cretaceous basin-margin rudist buildups of the Mesopotamian Basin, southern Iraq, with consideration of possible hydrocarbon stratigraphic entrapment. *Cretaceous Research*, 26(2), 213-224.
- Schlager, W., 2005. Carbonate Sedimentology and Sequence Stratigraphy. *Geological Magazine*, 145(1), 156-156. DOI: 10.1017/S0016756807004177
- Sepehr, M., Cosgrove, J.W., 2005. Role of the Kazerun Fault Zone in the formation and deformation of the Zagros Fold-Thrust Belt, Iran. *Tectonics*, 24(5), TC5005. DOI: 10.1029/2004TC001725
- Sharland, P.R., Archer, R., Casey, D.M., 2001. Chapter 4: Maximum Flooding Surfaces. In: Sharland, P.R., Archer, R., Casey, D.M., Davies, R.B., Hall, S.H., Heward, A.P., Horbury, A.D., Simmons, M.D. (eds.). *Arabian Plate Sequence Stratigraphy: GeoArabia*. Manama, Bahrain, Gulf PetroLink, 261-278.
- Sharp, I., Gillespie, P., Morsalnezhad, D., Taberner, C., Karpuz, R., Vergés, J., Horbury, A., Pickard, N., Garland, J., Hunt, D., 2010. Stratigraphic architecture and fracture-controlled dolomitization of the Cretaceous Khami and Bangestan groups: an outcrop case study, Zagros Mountains, Iran. In: Van Buchem, F., Gerdes, K., Esteban, M. (eds.). *Mesozoic and Cenozoic Carbonate Systems of the Mediterranean and the Middle East: Stratigraphic and Diagenetic Reference Models*. Geological Society of London, 329 (Special Publications), 343-396.
- Sherkati, S., Letouzey, J., 2004. Variation of structural style and basin evolution in the central Zagros (Izeh zone and Dezful Embayment), Iran. *Marine and Petroleum Geology*, 21(5), 535-554.
- Sherkati, S., Molinaro, M., Frizon De Lamotte, D., Letouzey, J., 2005. Detachment folding in the Central and Eastern Zagros fold-belt (Iran): salt mobility, multiple detachments and late basement control. *Journal of Structural Geology*, 27(9), 1680-1696.
- Sun, S.Q., Estaban, M., 1994. Paleoclimatic controls on sedimentation, diagenesis, and reservoir quality: lessons from Miocene carbonates. *American Association of Petroleum Geologists Bulletin*, 78(4), 519-543.
- Van Buchem, F.S.P., Razin, P., Homewood, P.W., Philip, J.M., Eberli, G.P., Platel, J.P., Roger, J., Eschard, R., Desaubliaux, G.M.J., Boisseau, T., Leduc, J.P., Labourdette, R., Cantaloube, S., 1996. High resolution sequence stratigraphy of the Natih Formation (Cenomanian/Turonian) in Northern Oman: distribution of source rocks and reservoir facies. *GeoArabia*, 1(1), 65-91.
- Van Buchem, F.S.P., Razin, P., Homewood, P.W., Otterboom, W.H., Philip, J., 2002. Stratigraphic organization of carbonate ramps and organic-rich intra-shelf basins: Natih Formation (middle Cretaceous) of northern Oman. *American Association of Petroleum Geologists Bulletin*, 86(1), 21-54.

- Van Buchem, F.S.P., Simmons, M., Droste, H., Davies, R.R.B., 2011. Late Aptian to Turonian stratigraphy of the eastern Arabian Plate - depositional sequences and lithostratigraphic nomenclature. *Petroleum Geoscience*, 17(3), 211-222.
- Verges, J., Goodarzi, M.G.H., Emami, H., Karpuz, R., Efstathiou, J., Gillespie, P., 2009. Multiple detachment folding in Pusht-e Kuh Arc, Zagros: Role of mechanical stratigraphy. In: McClay, K., Shaw, J., Suppe, J. (eds.). *Thrust fault-related folding*. American Association of Petroleum Geologists Memoir, 94, 1-26.
- Weidlich, O., 2010. Meteoric diagenesis in carbonates below karst unconformities: heterogeneity and control factors. In: Van Buchem, F.S.P., Gerdes, K.D., Esteban, M. (eds.). *Mesozoic and Cenozoic carbonate systems of the Mediterranean and the Middle East: Stratigraphic and diagenetic reference models*. Geological Society London, 329 (Special Publications), 291-315. DOI: 10.1144/SP329.12
- Wilson, J.L., 1975. *Carbonate Facies in Geologic History*. New York, Springer-Verlag, 471 pp.
- Wynd, J.G., 1965. *Biofacies of the Iranian Oil Consortium Agreement Area*. Iranian Offshore Oil Company Report, 1082, 89pp.

**Manuscript received September 2017;
revision accepted June 2018;
published Online July 2018.**

ELECTRONIC APPENDIX

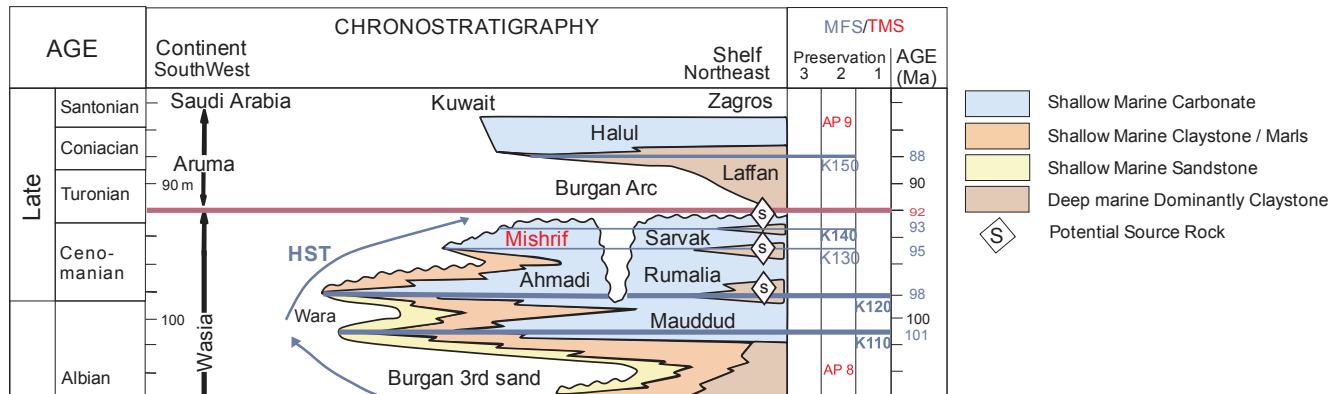


FIGURE I. Chronostratigraphic chart of the mid- and late-Cretaceous in the Arabian Plate (modified after Sharland *et al.*, 2001).

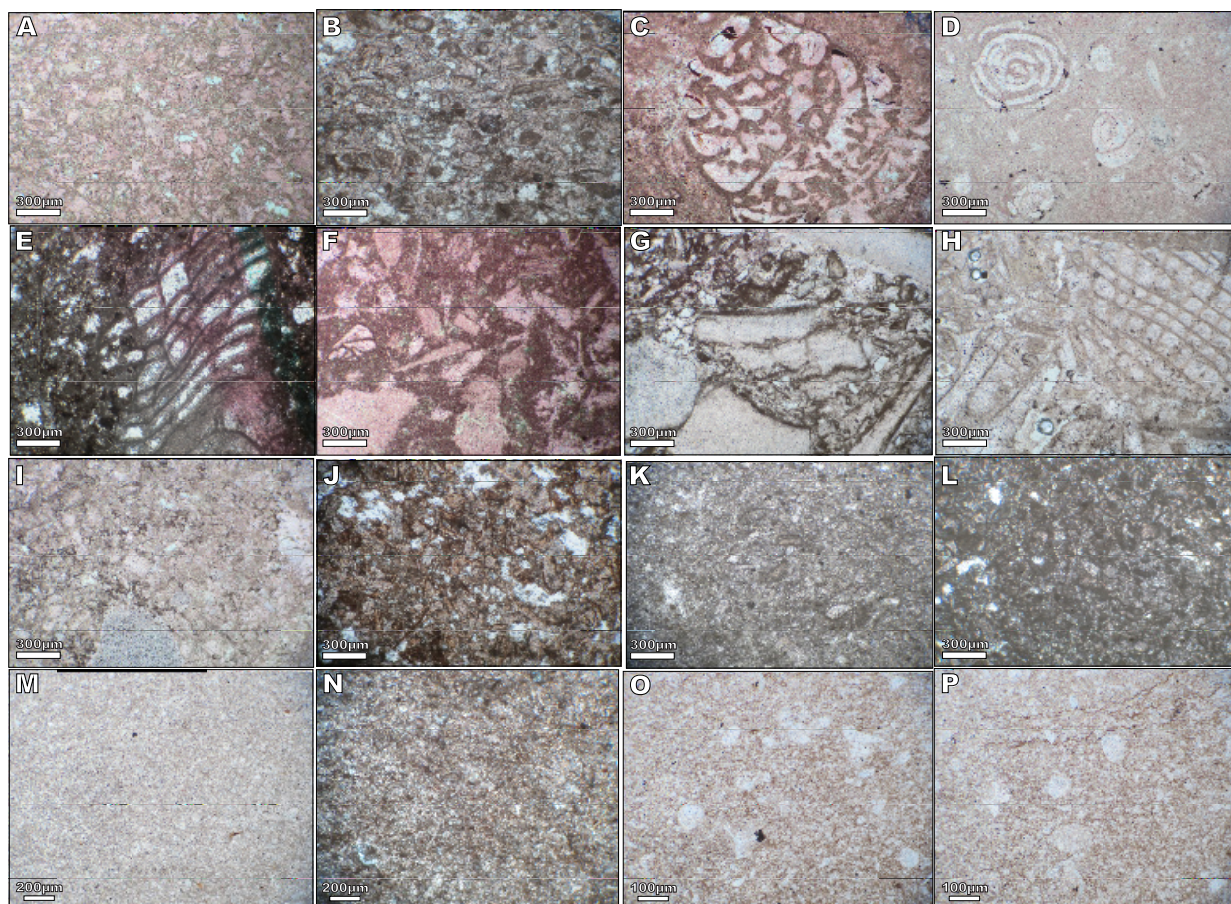


FIGURE II. Identified microfacies of the Mishrif Fm. in the studied fields. A-B) RMF1, peloidal/bioclastic packstone to grainstone. C-D) RMF, large benthic foraminifera wackestone with rudist debris. E-F) RMF3, rudist debris floatstone. G-H) RMF4, rudist rudstone. I-J) RMF5, peloid bioclast packstone/wackestone. K-L) RMF6, peloid bioclast wackestone/mudstone. M-N) RMF7, mudstone. O-P) RMF8, planktonic foraminifera wackestone/mudstone. All figures are in Plane Polarized Light (PPL) and X5.

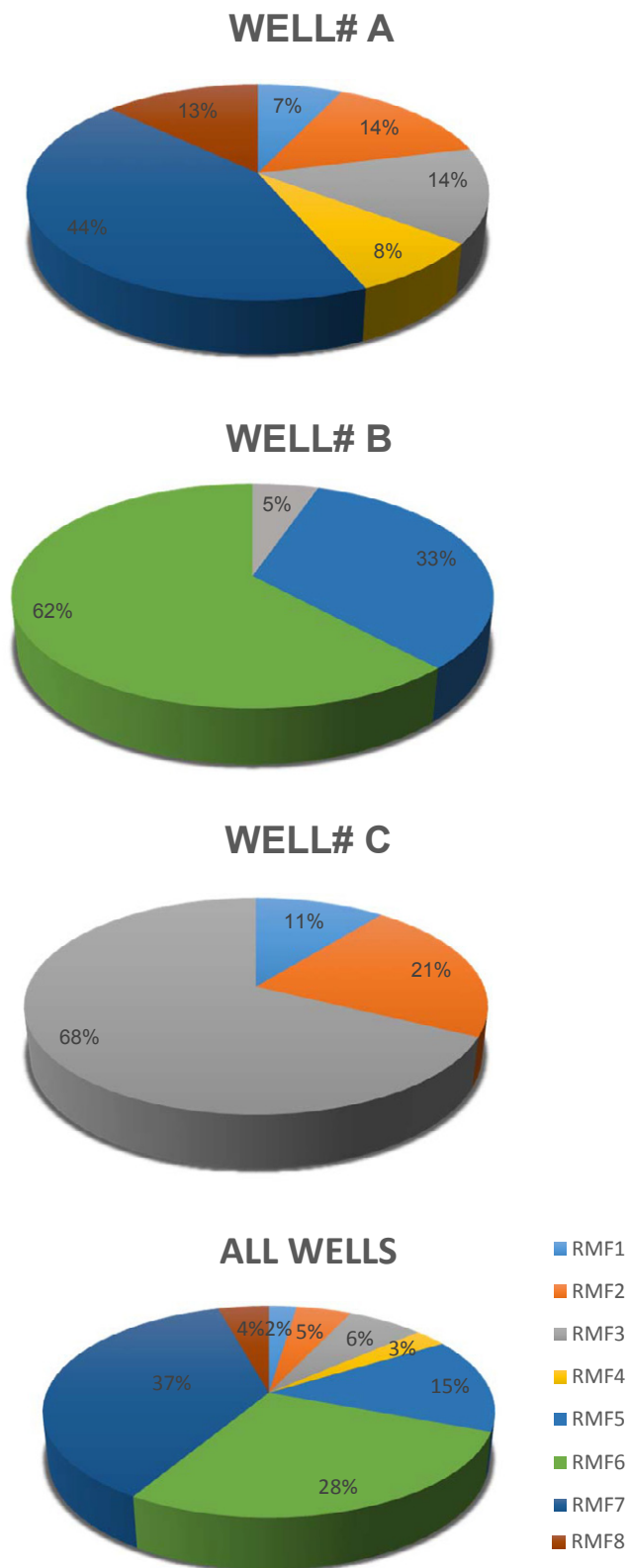


FIGURE III. Pie diagrams showing the frequency (percent) of different microfacies (RMFs) identified in three studied fields.

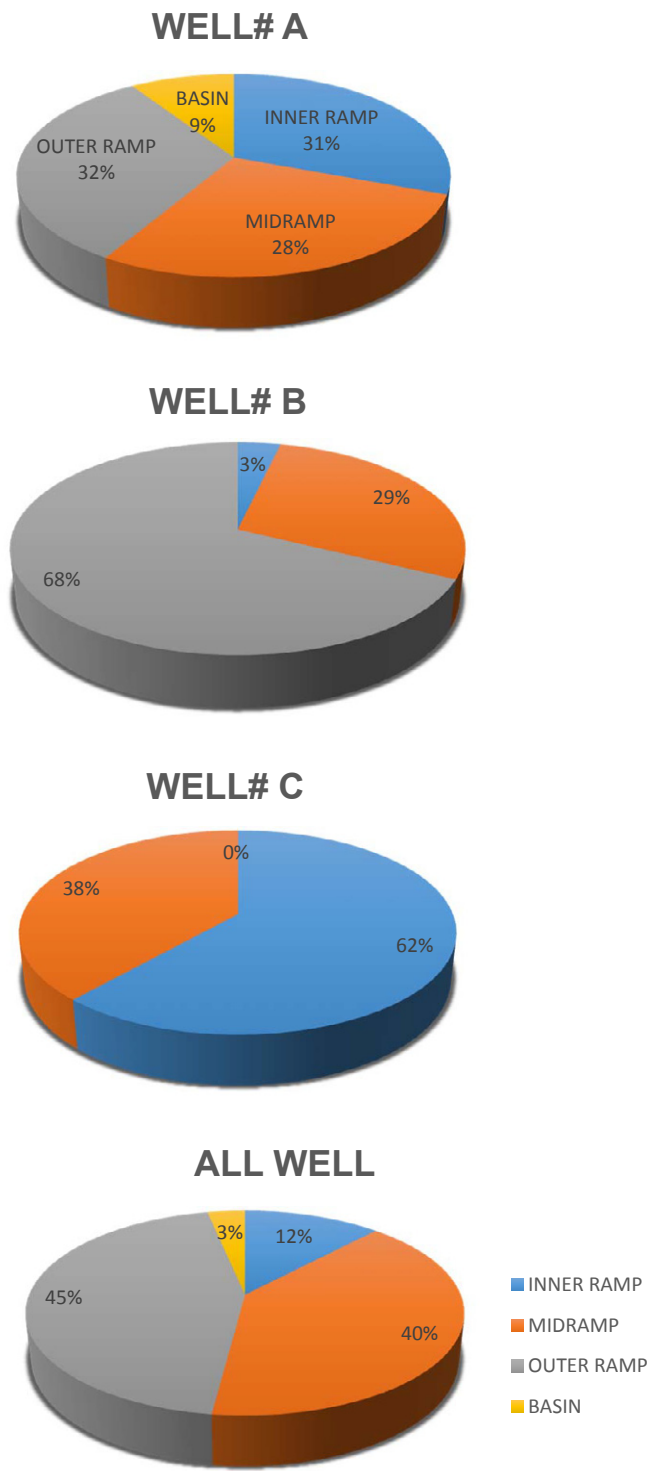


FIGURE IV. Pie diagrams showing the frequency (percent) of different facies belts (FBs) identified in three studied fields.

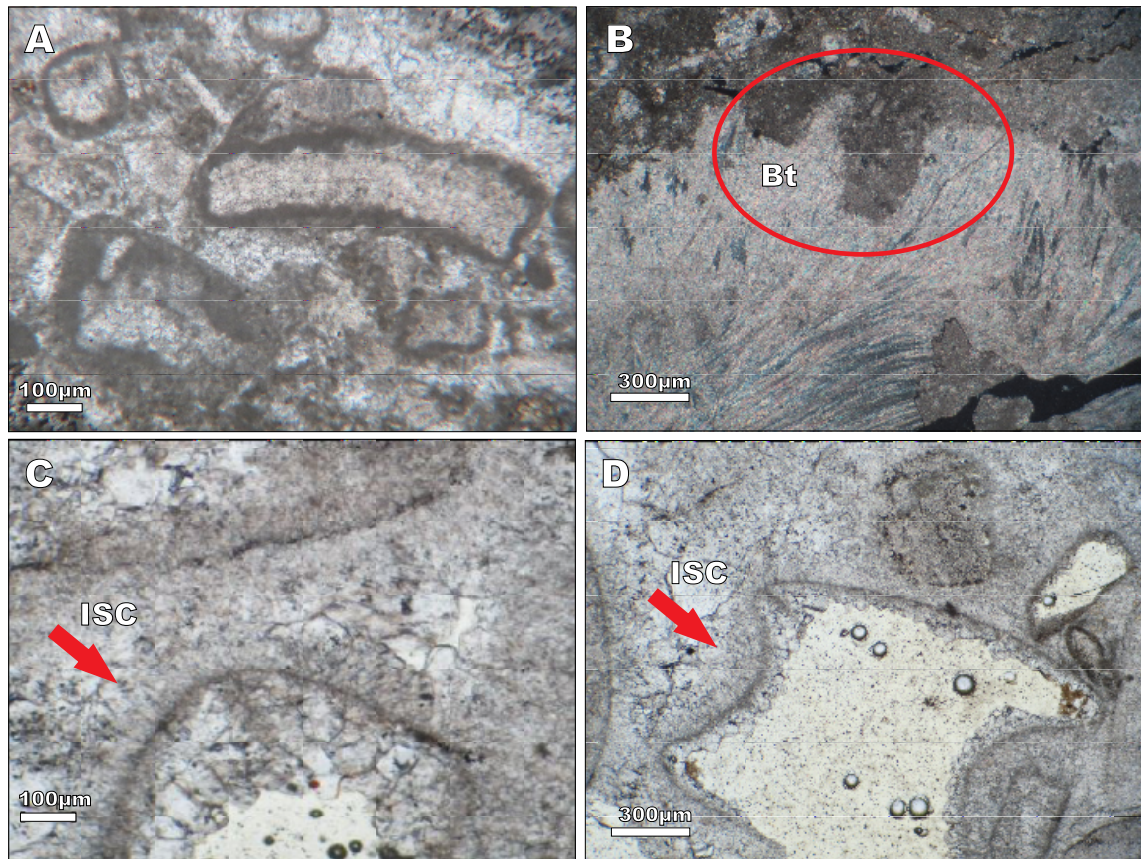


FIGURE V. Marine environment diagenetic processes. A) Micritization. B) Bioturbation (boring). C- D) Thin isopachous microcrystalline calcite cement. (All in PPL, X5).

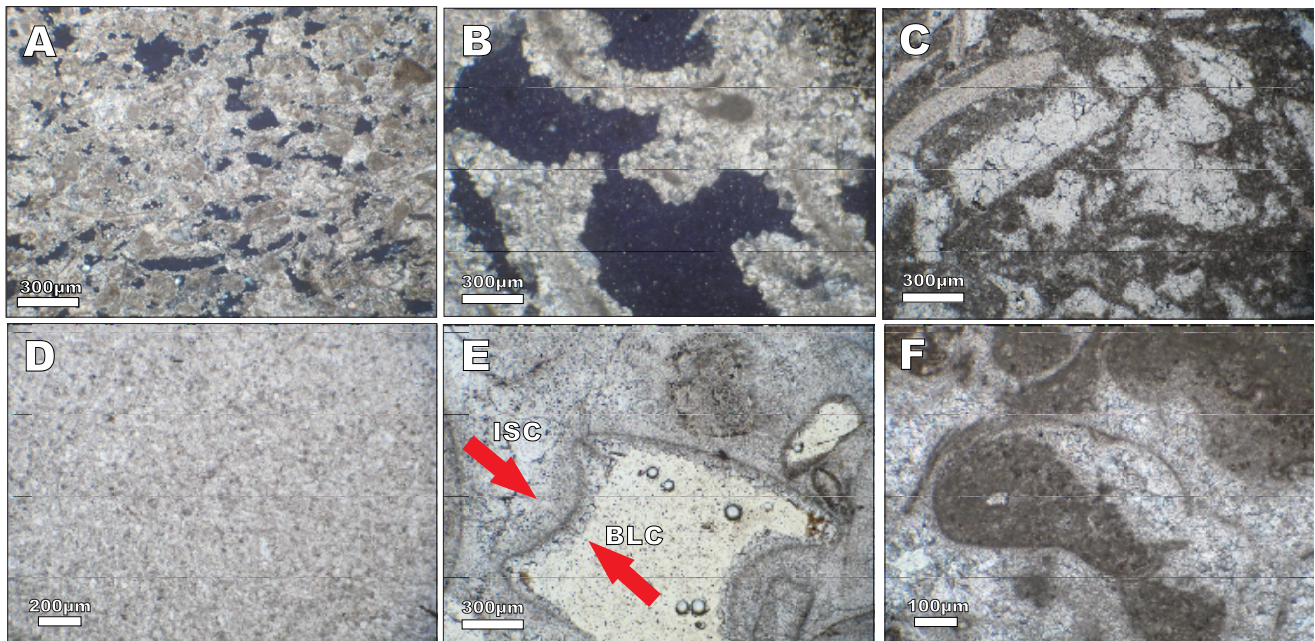


FIGURE VI. Meteoric environment diagenetic processes. A-B) Meteoric dissolution (in xpl and X5). C-D) Neomorphism (in PPL and X5). E) Meteoric cementation (in PPL and X5). F) Geoptal fabric (in PPL and X5).

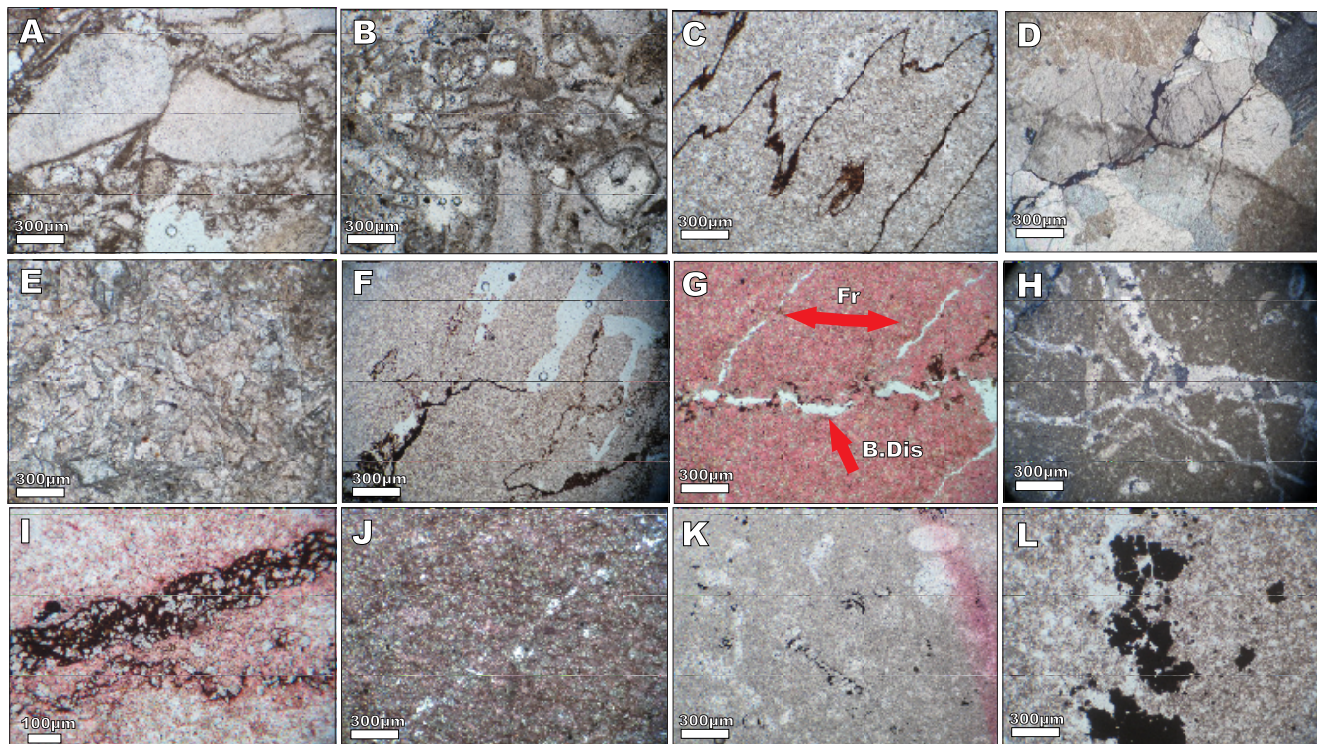


FIGURE VII. Burial environment diagenetic processes. A-B) Physical compaction. C) High-amplitude stylolite. D-E) Burial cementation with coarse crystal and sharp cleavages. F-G) Burial dissolution, occurrence of solution on stylolite. G-H) Fracturing (open and filled). I) Dolomitization related to solution seams with fine- to medium-size and euhedral to subhedral crystals. J) Sparse dolomitization with very fine- to medium-size and euhedral to subhedral crystals in micrite of mud-dominated facies. K-L) Secondary pyritization. (All in PPL and X5).

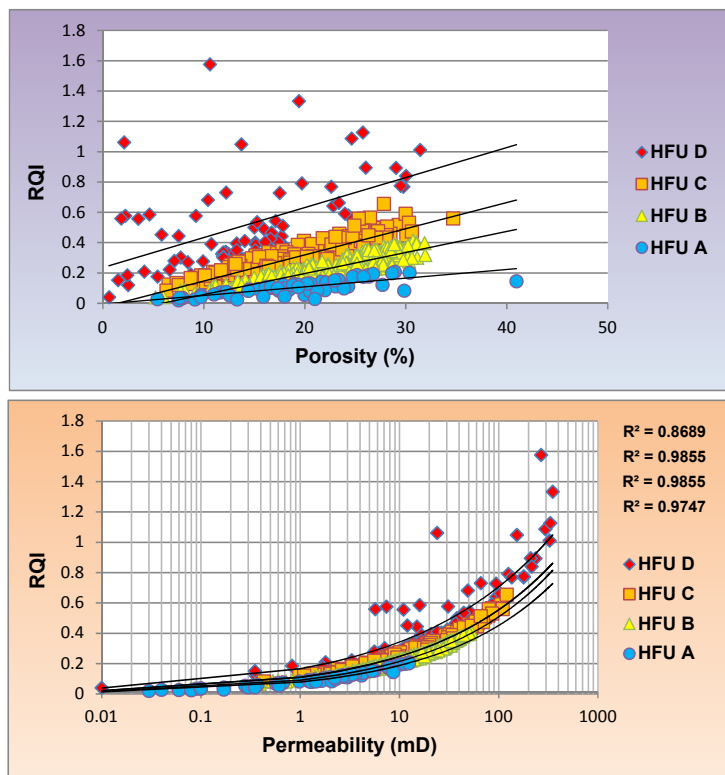


FIGURE VIII. Relationship between Reservoir Quality Index (RQI) with porosity (A) and permeability (B) for different hydraulic flow units in the reservoir.

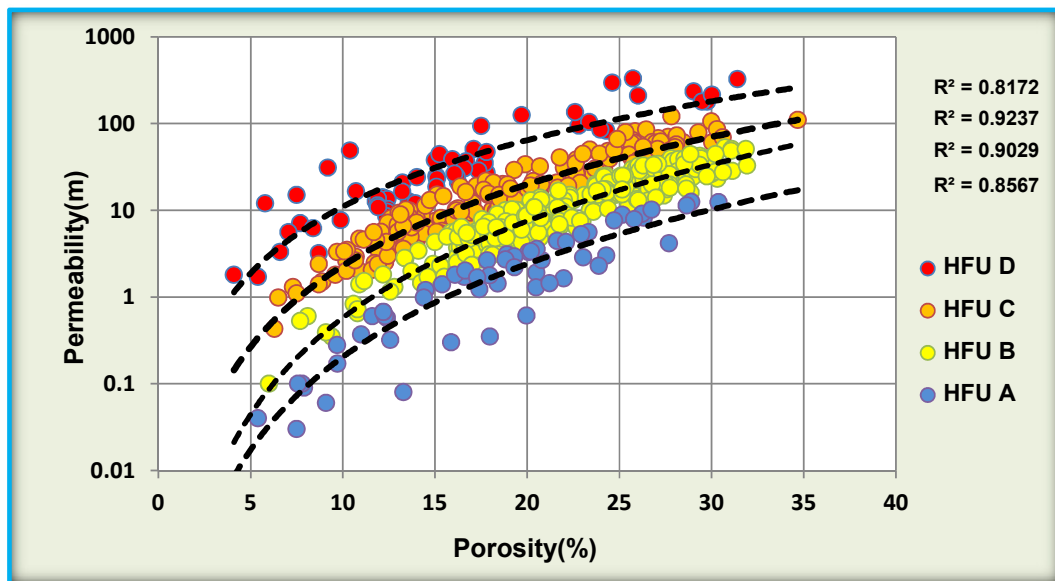


FIGURE IX. Distribution of different hydraulic flow units on porosity and permeability plot for the Mishrif reservoir.

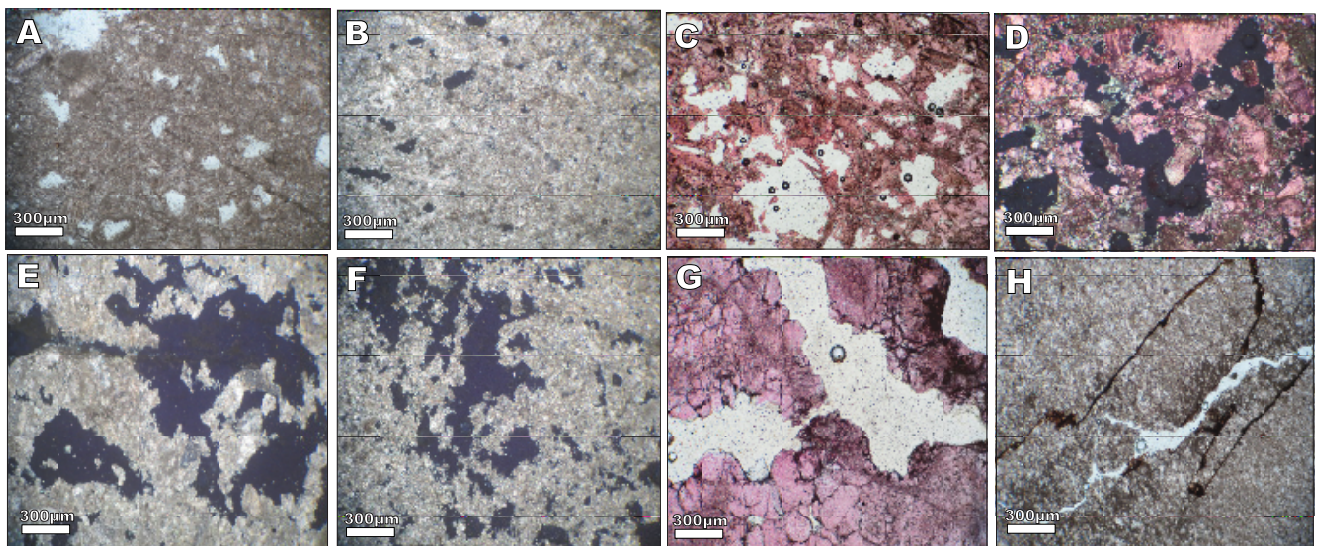


FIGURE X. A-B) HFUA, with high-porosity and low-permeability and non-attached vugs and moldic pores resulted from meteoric dissolution. C-D) HFUB, with intermediate porosity and permeability and most of the pore spaces are touching vugs. E-F) HFUC (are similar to HFUB). G-H) HFUD, with high-quality especially with high-permeability and low-porosity related touch and non-touching micro vugs to because of open fracture and burial dissolution. (A, C, G and H are in PPL and X5. B, D, E and F are Double (or crossed) Polarized Light (XPL) and X5).

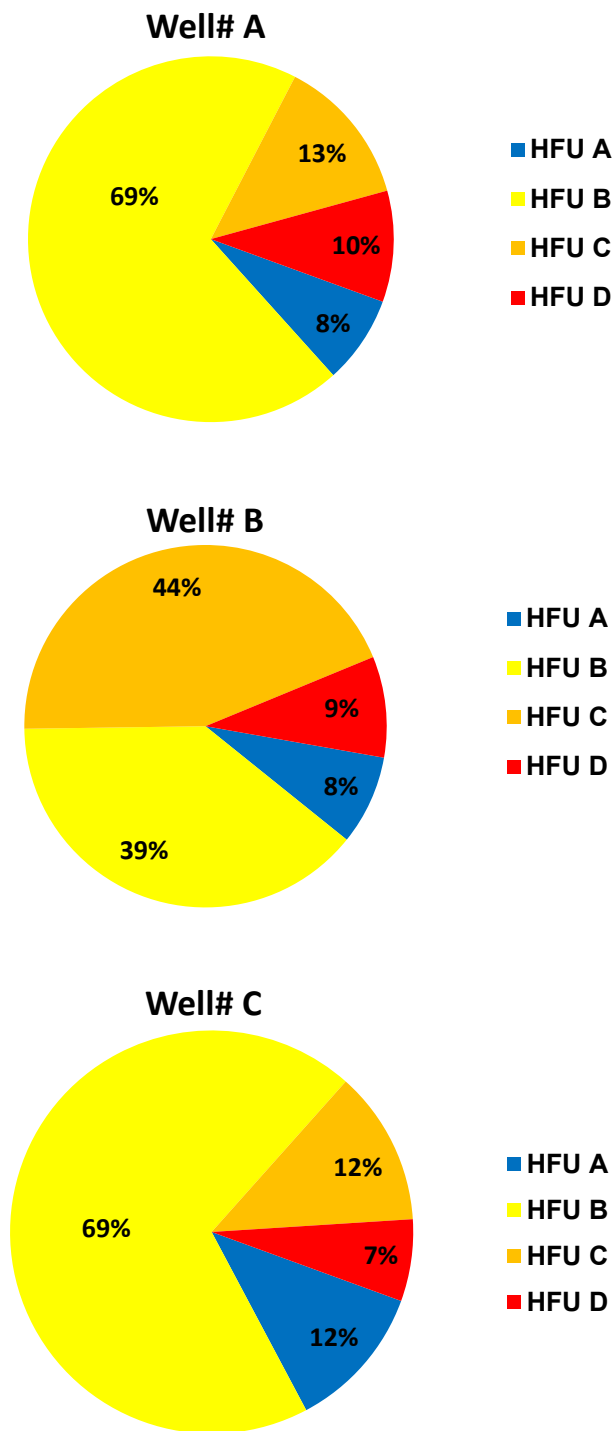


FIGURE XI. Pie diagram showing the frequency of the identified flow units in the studied wells (A, B and C).